

# Optimal fermion-qubit mappings

Mitchell Chiew<sup>1</sup> and Sergii Strelchuk<sup>1</sup>

<sup>1</sup> DAMTP, Centre for Mathematical Sciences, University of Cambridge, Cambridge CB30WA, UK

## Abstract

Simulating fermionic systems on a quantum computer requires a high-performing mapping of fermionic states to qubits. The key characteristic of an efficient mapping is its ability to translate local fermionic interactions into qubit interactions. This has strong implications both on the number of qubits as well as the gate cost of simulations. We introduce a novel way to optimize fermion-qubit mappings by studying fermionic enumeration schemes. Finding an efficient enumeration scheme allows one to increase the locality of the target qubit Hamiltonian without expending any additional resources. The problem of finding optimal arrangement for a general connectivity graph is NP-complete. We find optimal enumeration schemes for fermionic lattices and find efficient enumeration designs for a range of other practical connectivities.

## 1 Introduction

Simulating physical systems is one of the most promising applications of quantum computers. Fermionic systems, encountered in many fields of theoretical and experimental physics, ranging from quantum chemistry to condensed matter to quantum field theories, pose a complex, often intractable computational challenge when studied with the aid of classical computers. These include, for example, the electronic structure problem, studying properties of gauge theories that govern strong interactions between quarks and gluons, determining ground state properties of fermionic Hamiltonians and many others.

There has been a number of recent developments in quantum computing that make the above questions feasible [1, 2, 3, 4, 5, 6, 7]. However, many of these approaches [1, 7] rely on phase estimation [8, 9] and in turn require an impractically large number of qubits and quantum gates in order to keep the register of the quantum computer coherent [10]. Even those algorithms designed for near-term quantum computers, such as variational quantum eigensolvers [10, 11, 2], are beyond the reach of current technology. Furthermore, studying fermionic systems in 2D or 3D greatly amplifies these difficulties because of the overwhelming number local fermionic interactions that become increasingly non-local once mapped in the qubit picture. The first mapping in 2D was introduced by Verstraete and Cirac [12], and despite giving rise to highly non-local terms is still being widely used.

To bring the problem of fermionic simulation closer to meeting constraints of near-term quantum technology, it is crucially important to establish protocols that find optimal (in a certain well-defined sense) tradeoffs between the locality of the fermionic interactions and the locality of the corresponding interactions once mapped onto qubits. This is a complex challenge that largely has

not been met with much progress because the formalization of simulating fermionic interactions in complexity-theoretic sense has has been extraordinarily difficult.

One can break down all quantum algorithms for fermionic simulation into three sequential steps: initialising the quantum qubit register, applying unitary gates, and measuring the result to obtain an estimate for the desired molecular property or other quantity of interest. Within this framework, algorithms may encode the fermionic Hamiltonian via first or second quantisation. Fermi-Dirac statistics impose asymmetry on fermionic systems' wavefunctions, and using first quantisation of the system's Hamiltonian, one can incorporate this asymmetry into the qubit basis itself or use the qubits to directly encode the wavefunction into real-time and real-space [1, 7, 4, 3]. Second quantisation encodes the asymmetry into the qubit operators rather than the quantum states [2]. This method necessitates a fermion-qubit mapping, to preserve the properties of fermionic creation and annihilation operators.

In our work, we focus on second quantisation because it provides a number of advantages over representations in the first quantisation [12, 13]. In the second quantisation picture Hamiltonians are made up of products of fermionic creation and annihilation operators; a quantum algorithm must map each term of the Hamiltonian into a sequence of unitary gates acting on qubits. This transforms the original problem into the  $k$ -local Hamiltonian problem, where the size of  $k$  depends on the choice of fermion-qubit mapping. While in general, the local Hamiltonian problem is QMA complete [14], numerous attempts to reduce the complexity of this problem include using additional auxiliary qubits [15, 12, 16] in improved fermion-qubit mappings. Auxiliary qubits decrease non-locality of the qubit Hamiltonian, substantially reducing the complexity, and making small instances of a problem within reach of fairly modest quantum computers.

The idea of spin-fermion mappings originates in the work of Jordan and Wigner almost a century ago [17]. In recent years, there has been a flurry of results that introduce new fermion-qubit mappings as well as generalize the existing ones to higher dimensions [18, 19, 15, 16, 20]. Nearly all of them work well in 1D, but experience impractically large overheads in higher dimensions. To address this, one may consider adding auxiliary qubits [12, 16].

One entirely overlooked aspect of fermion-qubit mappings in higher dimensions is the use of the underlying fermion enumeration scheme. While trivial in 1D, it has the potential to dramatically improve the locality of the mapping in 2D and above. The type of lattice and the method of numbering fermions opens up new avenues for optimizing fermion-qubit mappings. Examining enumeration schemes, and finding the most efficient ones we show how to increase the locality of the target qubit Hamiltonian without expending any additional resources. This directly translates into reductions for quantum gate count that correspond to hopping terms. In our work, we will consider several figures of merit. One such central quantity, the Pauli weight of a string of Pauli operations is the number of qubits involved in the string.

We relate the problem of optimising the simulation of hopping terms of fermionic Hamiltonians in 2D to the **Edgesum problem** from graph theory [21, 22, 23, 24]. We find that the optimal ancilla-free enumeration scheme corresponds to the optimal solution of the Edgesum problem. For regular fermionic lattice this directly improves locality and thus reduces the resources used by quantum algorithms by a constant factor ( $\approx 13.9\%$ ) compared to the S-pattern introduced by Verstraete and Cirac [12]. Surprisingly, our fermion-qubit mapping requires no additional resources – only a carefully selected enumeration scheme. Our construction relies on a special pattern investigated by Mitchison and Durbin in their seminal work [21]. We thus show that:

**Theorem 1** [Informal]

*Given a system of  $n = N^2$  fermions interacting in a square  $N \times N$  lattice, then the fermion*

enumeration scheme that follows Mitchison-Durbin pattern minimises the average Pauli weight of the hopping terms.

Our approach of choosing edgesum-minimising fermion enumeration schemes gives practical results beyond the case of the 2D lattice. For graphs of cellular arrangements of  $n$  fermions, ‘bespoke’ enumeration schemes perform better than naïve alternatives by a factor of  $\mathcal{O}(n^{1/4})$ , as Section 3.4 demonstrates. This implies that for particular families of graphs, it is highly likely that optimal enumeration scheme to produces quantum circuits orders of magnitude shallower than one-size-fits all enumeration schemes.

The structure of the paper is as follows: in Section 2 we provide a self-contained introduction to fermion-qubit mappings and their implications on the gate count further specialized to Jordan-Wigner mapping. It is then followed by results from complexity theory that will be used to prove our main result. In Section 3 we introduce fermion enumeration schemes, rigorous cost functions and show how to construct an optimal enumeration scheme in 2D. Finally, in Section 4 we put our findings in perspective and discuss further ways of improving fermion-qubit mappings.

## 2 Background

This section provides the necessary background for the Jordan Wigner transformation on fermionic systems in Sections 2.1–2.4, and details relevant graph problems and complexity theory in Section 2.5.

### 2.1 Canonical commutation relations

In order to describe a system of  $n$  fermions, it is necessary to label each fermion with an integer from 1 to  $n$ . This is the first step of any fermion-qubit mapping, and here we call it the process of choosing a *fermion enumeration scheme*. The fermionic system has a state space, known as *Fock space*, with the occupancy number basis  $\{|j_1, j_2, \dots, j_n\rangle \mid j_i \in \{0, 1\}\}$  where  $j_i$  denotes the occupancy of the  $i$ th fermion. The annihilation operators  $a_i$  act on the fermionic vector space as

$$a_i |j_1, j_2, \dots, j_{i-1}, 0, j_{i+1}, \dots, j_n\rangle = 0 \quad (1)$$

$$a_i |j_1, j_2, \dots, j_{i-1}, 1, j_{i+1}, \dots, j_n\rangle = (-1)^{\sum_{k=1}^{i-1} j_k} |j_1, j_2, \dots, j_{i-1}, 0, j_{i+1}, \dots, j_n\rangle, \quad (2)$$

while their Hermitian conjugates  $a_i^\dagger$  are the creation operators, and act on the system accordingly.

Equations 1 and 2 are equivalent to Equations 3,4,5, which are the *fermionic commutation relations* (CCRs):

$$\{a_j, a_k\} = 0 \quad (3)$$

$$\{a_j^\dagger, a_k^\dagger\} = 0 \quad (4)$$

$$\{a_j, a_k^\dagger\} = \delta_{jk} \mathbf{1}. \quad (5)$$

### 2.2 Fermion–qubit mappings

Consider a general Hamiltonian  $H$  which encodes the dynamics of fermionic system:

$$H = \sum_{\alpha} h_{\alpha} O_{\alpha}, \quad (6)$$

where each  $O_\alpha$  is the product of an equal number of creation and annihilation operators, and the complex coefficients  $h_\alpha$  ensure that  $H$  is Hermitian. To simulate the  $n$  fermions, we suppose that we have  $m \geq n$  qubits at our disposal. The state of the qubit system can be written in terms of the basis  $\{|l_1, l_2, \dots, l_m\rangle \mid l_i \in \{0, 1\}\}$ , where  $l_i$  denotes the value of the binary observable (say,  $z$ -component of spin) of the  $i$ th qubit. Developing a fermion-qubit mapping is tantamount to finding unitary operators  $\mathbb{A}_i \in U(m)$  such that  $\{\mathbb{A}_i^\dagger, \mathbb{A}_j\} = \delta_{ij} \mathbf{1}$  and  $\{\mathbb{A}_i^{(\dagger)}, \mathbb{A}_j^{(\dagger)}\} = 0$ , for  $i, j \in \{1, 2, \dots, n\}$ .

Table 1 summarises the defining properties of fermionic systems and their analogues in qubit systems and Figure 1 illustrates the most general transformation that is attained by fermion-qubit mappings. All known fermion-qubit mappings in the literature are a subset of the template described in the above table and the figure.

The most widely-used fermion-qubit mappings, such as the Jordan-Wigner [17] and Bravyi-Kitaev [25] transformations, simulate  $n$  fermions with  $n$  qubits. Mappings that use  $m > n$  qubits, e.g. [16, 15] transform Hamiltonian terms into chains of Pauli spin operators ( $\sigma^x, \sigma^y, \sigma^z$ ) and reduce the lengths of these chains with stabilisers involving auxiliary qubits. A considerable repertoire of fermion-qubit mappings has developed in recent years, each with its own strengths and weaknesses.

Property System	Basis states	Fundamental operators
$n$ fermions	$ j_1, j_2, \dots, j_n\rangle$ $j_i = \text{occupancy}$	Ladder operators $a_i, a_j^\dagger$ satisfying $\{a_i, a_j^\dagger\} = \delta_{ij} \mathbf{1}$ , $\{a_i^{(\dagger)}, a_j^{(\dagger)}\} = 0$ ; Physical operators $\propto a_i^\dagger a_j + a_j^\dagger a_i$
$m \geq n$ qubits	$ l_1, l_2, \dots, l_m\rangle$ $l_i = \text{spin}$	Unitary matrices $\mathbb{A}_i, \mathbb{A}_j^\dagger$ , for $i = 1, \dots, n$ , satisfying $\{\mathbb{A}_i, \mathbb{A}_j^\dagger\} = \delta_{ij} \mathbf{1}$ , $\{\mathbb{A}_i^{(\dagger)}, \mathbb{A}_j^{(\dagger)}\} = 0$

Table 1: Basic building blocks of fermionic systems, and the equivalent properties that must apply to a system of qubits in order for it to simulate the fermions.

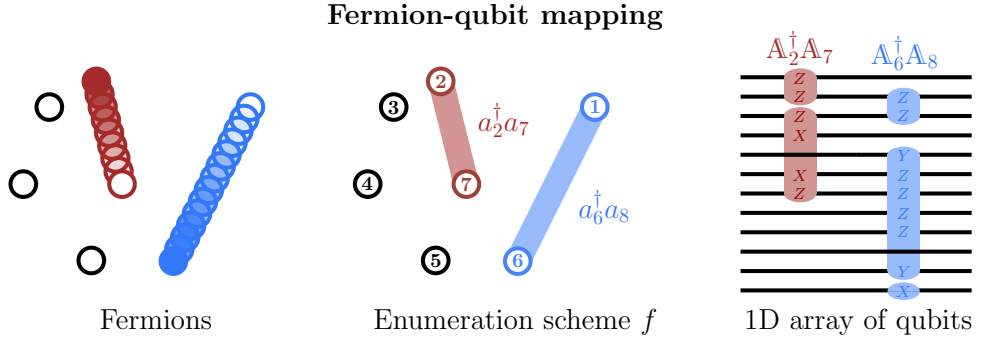


Figure 1: A fermion-qubit mapping uses a fermion enumeration scheme to describe interactions, such as  $a_i^\dagger a_j$ . Via the transformations  $a_i \mapsto \mathbb{A}_i$ , the fermion-qubit mapping replicates the algebra of the CCRs on a system of  $m \geq n$  qubits.

### 2.3 The Jordan-Wigner transformation

The Jordan-Wigner transformation uses  $m = n$  qubits and arises naturally by constructing

$$\sigma^+ := \frac{1}{2}(\sigma^x - i\sigma^y) = \frac{1}{2}(X - Y) = |1\rangle\langle 0| \quad (7)$$

$$\sigma^- := \frac{1}{2}(\sigma^x + i\sigma^y) = \frac{1}{2}(X + Y) = |0\rangle\langle 1|, \quad (8)$$

which behave somewhat like creation-annihilation operators in ket-bra form. Here,  $X = \sigma^x$  and  $Y = i\sigma^y$  as is the standard notation. While  $\{\sigma^+, \sigma^-\} = \mathbf{1}$ , across multiple qubits when  $i \neq j$  we have  $\{\sigma_i^+, \sigma_j^-\} = |01\rangle\langle 10|_{i,j} \neq 0$ , where the subscript  $i$  denotes action on the  $i$ th qubit. Thus,  $\sigma_i^-$  and  $\sigma_j^+$  alone cannot replicate the CCRs of the operators  $a_i$ , and  $a_j^\dagger$ .

The Jordan-Wigner transformation defines  $\mathbb{A}_i$  and  $\mathbb{A}_j^\dagger$  via

$$a_i \mapsto \mathbb{A}_i = \left( \bigotimes_{k=1}^{i-1} \sigma_k^z \right) \sigma_i^- \quad (9)$$

$$a_j^\dagger \mapsto \mathbb{A}_j^\dagger = \left( \bigotimes_{k=1}^{i-1} \sigma_k^z \right) \sigma_j^+. \quad (10)$$

Using the anticommutation relations  $\{\sigma_i^\pm, \sigma_i^z\} = 0$ ,

$$\{\mathbb{A}_i, \mathbb{A}_j^\dagger\} = \{\sigma_i^-, \sigma_j^z\} \left( \bigotimes_{k=i+1}^{j-1} \sigma_k^z \right) \sigma_j^+ = 0, \quad (11)$$

where  $j > i$ , as is required of a fermion-qubit mapping.

In our work we confine our discussion to Jordan-Wigner type mappings, which exhibit a direct and intuitive correlation between fermions and qubits. The correlation is thus:  $\mathbb{A}_i$  and  $\mathbb{A}_j^\dagger$  naturally act on the spin basis  $\{|l_1, l_2, \dots, l_n\rangle \mid l_i \in \{0, 1\}\}$  in exactly the same way that the fermionic creation

and annihilation operators  $a_i$  and  $a_j^\dagger$  act on the Fock basis  $\{|j_1, j_2, \dots, j_n\rangle \mid j_i \in \{0, 1\}\}$ . That is,  $l_i = j_i$ . This is in contrast to other fermion-qubit mappings – for example in the case of the Bravyi-Kitaev transformation [25], the operators  $A_i$  and  $A_j^\dagger$  act on a basis for qubit space  $\{|b_1, b_2, \dots, b_n\rangle \mid b_i \in \{0, 1\}\}$ , where  $b_i = \sum_k [\mathbf{B}]_{ik} j_k$  and  $\mathbf{B}$  is a specific invertible matrix.

## 2.4 Jordan-Wigner transformation of Hamiltonian hopping terms

Typical molecular electronic Hamiltonians  $H$  acting on  $n$  fermions have the form

$$H = \sum_{\alpha\beta} (h_{\alpha\beta}) a_\alpha^\dagger a_\beta + \frac{1}{2} \sum_{\alpha\beta\gamma\delta} (h_{\alpha\beta\gamma\delta}) a_\alpha^\dagger a_\beta^\dagger a_\gamma a_\delta, \quad (12)$$

where the indices  $\alpha, \beta, \gamma, \delta$  are unordered labels for the  $n$  fermions. The complex coefficients  $h_{\alpha\beta}$  and  $h_{\alpha\beta\gamma\delta}$  are respectively one- and two-electron overlap integrals, such that  $H$  is Hermitian. The Hamiltonian in Equation 12 is an example of a Fermi-Hubbard model and conserves particle number. As the molecular system involves electrons, which are spin- $\frac{1}{2}$  fermions, the indices in the summations both run through the different spin orbitals of each electron and also traverse over all of the electrons.

The Jordan-Wigner transformation uses a fermion enumeration scheme  $f$  to convert the indices  $\alpha, \beta, \gamma, \delta$  into numerical indices  $i, j, k, l \in \{1, 2, \dots, n\}$ . It then transforms the single-electron excitation terms of  $H$ , known as *hopping terms*, into strings of Pauli gates:

$$a_i^\dagger a_i \mapsto \frac{1}{2} (\mathbf{1}_i - \sigma_i^z) = \frac{1}{2} (\mathbf{1}_i - Z_i) \quad (13)$$

$$a_i^\dagger a_j \mapsto \sigma_i^+ \left( \bigotimes_{k=i+1}^{j-1} \sigma_k^z \right) \sigma_j^- = \frac{1}{2} (X_i - Y_i) \left( \bigotimes_{k=i}^{j-1} Z_k \right) \frac{1}{2} (X_j + Y_j), \quad (14)$$

where  $i < j$  in Equation 14, and  $Z = \sigma^z$ . Figure 2 visualises how the Jordan-Wigner transformation maps the hopping terms in a fermionic system into Pauli strings. Here the fermions have a connectivity graph  $G_F$ , which means the Hamiltonian only includes the hopping terms  $a_\alpha^\dagger a_\beta$  where  $(\alpha, \beta)$  is an edge of  $G_F$ .

After using an enumeration scheme for the fermions, Figure 3 demonstrates the transformation of hopping terms  $a_2^\dagger a_7$  and  $a_5^\dagger a_4$ . However, these hopping terms would not feature in a Hamiltonian without appearing alongside their complex conjugate terms.

Indeed, to ensure that  $H$  is Hermitian, in any Hamiltonian  $H$  the term  $h_{ij} a_i^\dagger a_j$  will always appear alongside its conjugate term  $(h_{ij})^* a_j^\dagger a_i$ . Thus it is no less complete a description of the fermionic system to neglect Equation 14 and instead only consider

$$h_{ij} a_i^\dagger a_j + (h_{ij})^* a_j^\dagger a_i \mapsto \frac{\text{Re}(h_{ij})}{2} \left( \bigotimes_{k=i+1}^{j-1} \sigma_k^z \right) (\sigma_i^x \otimes \sigma_j^x + \sigma_i^y \otimes \sigma_j^y) + \frac{\text{Im}(h_{ij})}{2} \left( \bigotimes_{k=i+1}^{j-1} \sigma_k^z \right) (\sigma_i^y \otimes \sigma_j^x - \sigma_i^x \otimes \sigma_j^y) \quad (15)$$

$$= \frac{\text{Re}(h_{ij})}{2} \left( \bigotimes_{k=i+1}^{j-1} Z_k \right) (X_i \otimes X_j - Y_i \otimes Y_j) + \frac{i \text{Im}(h_{ij})}{2} \left( \bigotimes_{k=i+1}^{j-1} Z_k \right) (Y_i \otimes X_j - X_i \otimes Y_j). \quad (16)$$

In the case when the coefficients of the grouped terms are  $h_{ij} = (h_{ij})^* = 1$ , the transformation is simply

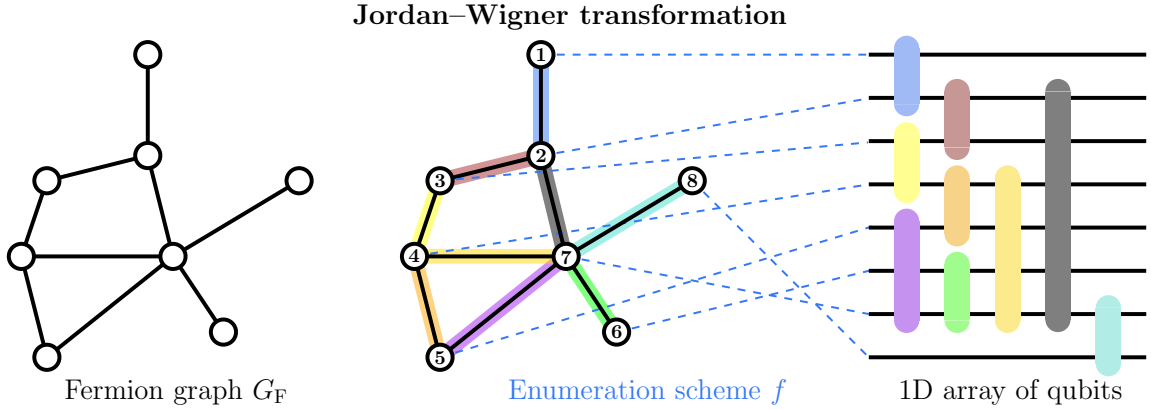


Figure 2: The Jordan-Wigner transformation converts an  $n$ -fermion Hamiltonian into strings of unitary Pauli gates on  $n$  qubits. Here, the graph  $G_F$  represents the single-fermion hopping interactions of the Hamiltonian.

$$a_i^\dagger a_j + a_j^\dagger a_i \longmapsto \frac{1}{2} \left( \bigotimes_{k=i+1}^{j-1} \sigma_k^z \right) (\sigma_i^x \otimes \sigma_j^x + \sigma_i^y \otimes \sigma_j^y) = \frac{1}{2} \left( \bigotimes_{k=i+1}^{j-1} Z_k \right) (X_i \otimes X_j - Y_i \otimes Y_j). \quad (17)$$

Figure 4 illustrates the conversion of conjugate hopping terms of the form of Equation 17 into quantum circuits.

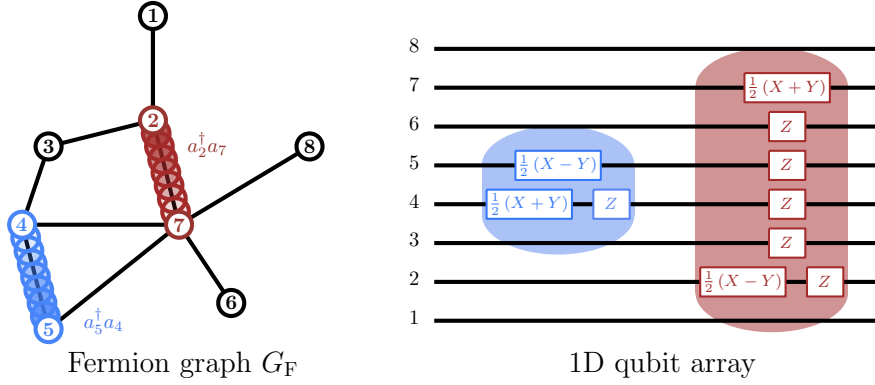


Figure 3: **Left:** representation of individual terms  $a_2^\dagger a_7$  and  $a_5^\dagger a_4$  in a fermionic Hamiltonian describing an unstructured system of fermions. **Right:** Jordan-Wigner transform of these terms into strings of Pauli operators acting on qubits.

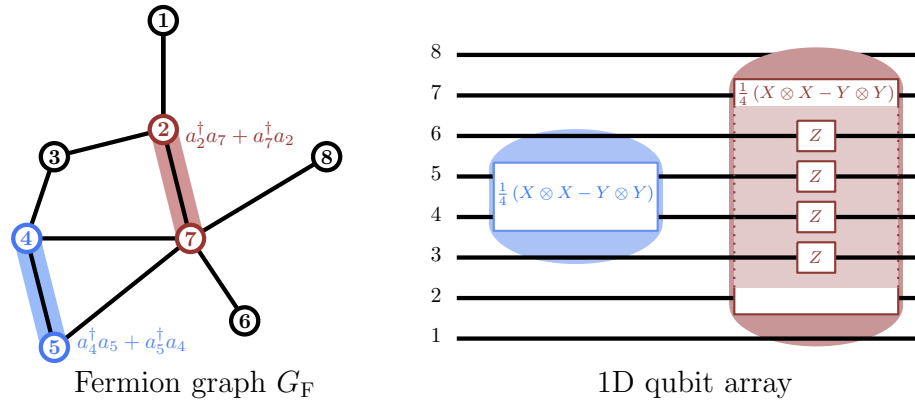


Figure 4: **Left:** as the Hamiltonian is Hermitian, every individual term of the form  $a_i^\dagger a_j$  can pair with its Hermitian conjugate  $a_j^\dagger a_i$ . **Right:** Jordan-Wigner transform of the grouped terms  $a_i^\dagger a_j + a_j^\dagger a_i$  into strings of Pauli operators acting on qubits.

## 2.5 Complexity-theoretical preliminaries

We now introduce the necessary notation and the complexity theoretic problems that we needed to for our results.

We start from All problems will have some variation of the following ingredients:

1. A **graph**  $G = (V, E)$  with  $|V| = n$  vertices and edge set  $E \subseteq V \times V$ , and
2. a **weight function**  $w : E \rightarrow \mathbb{R}$  describing flows between vertices, and
3. a list  $L$  of possible **locations** for the vertices, and
4. a **distance function**  $d : L \times L \rightarrow \mathbb{R}$  describing the spatial separation between the locations.

The following are a list of graph problems relevant to the discussion in this paper. All problems have the objective of finding a surjective **assignment function**  $f : V \rightarrow L$  to place the vertices in locations so as to minimise a cost function.

### 2.5.1 NP-hard problems

The following problem was shown by Koopmans [26] to be NP-hard:

#### QUADRATIC ASSIGNMENT

**INSTANCE:** Graph  $G = (V, E)$ , weight function  $w : E \rightarrow \mathbb{R}$ , vertex locations  $L$ , distance function  $d : L \times L \rightarrow \mathbb{R}$ .

**PROBLEM:** Find the location assignment function  $f : V \rightarrow L$  in such a way as to minimise the cost function

$$C(f) = \sum_{(\alpha, \beta) \in E} w(\alpha, \beta) \cdot d(f(\alpha), f(\beta)) . \quad (18)$$

### 2.5.2 Problems that are at least NP-complete.

The following problems appear to generalise some NP-complete problems, however it is unknown if they are NP-hard or strictly NP-complete. It was first studied by Garey and Johnson 1974 [22]. Note that it is different to the “optimal linear arrangement” in their book [24]. This is a special case of the quadratic assignment problem: the weight function  $w$  is restricted to integer values, the vertex locations  $L$  are  $\{1, 2, \dots, n\}$ , and the distance metric is  $d(i, j) = |i - j|$ . According to Horton [27], it is not known whether the optimal linear arrangement problem as written here is in NP-hard or if it is strictly contained within NP-complete.

#### OPTIMAL LINEAR ARRANGEMENT

**INSTANCE:** Graph  $G = (V, E)$ , weight function  $w : E \rightarrow \mathbb{Z}$ .

**PROBLEM:** Find the enumeration scheme  $f : V \rightarrow \{1, 2, \dots, n\}$  that minimises the cost function

$$C(f) = \sum_{(\alpha, \beta) \in E} w(\alpha, \beta) \cdot |f(\alpha) - f(\beta)| . \quad (19)$$

The following problem was studied by Mitchison and Durbin [21], Garey and Johnson [23], and Juvan and Mohar [28]. It is a special case of the optimal linear arrangement problem: its weight function is  $w(\alpha, \beta) = |f(\alpha) - f(\beta)|^{p-1} \in \mathbb{Z}$ . This problem is NP-complete for  $p = 1$  [22],  $p = 2$  [29] and  $p \rightarrow \infty$  [27]. One could also consider the broader class of problems where  $p \in \mathbb{R}$ , as done by Mitchison and Durbin [21]. These problems are likely to be at least as hard as their integer- $p$  equivalents.

#### MINIMUM $p$ -SUM

**INSTANCE:** Graph  $G = (V, E)$ , integer  $p \in \mathbb{Z}$ .

**PROBLEM:** Find the enumeration scheme  $f : V \rightarrow \{1, 2, \dots, n\}$  that minimises the cost function

$$C^p(f) = \left( \sum_{(\alpha, \beta) \in E} |f(\alpha) - f(\beta)|^p \right)^{1/p}. \quad (20)$$

#### 2.5.3 NP-complete problems.

The following problem was introduced in [22]:

#### SIMPLE OPTIMAL LINEAR ARRANGEMENT (also known as EDGESUM, MINIMUM 1-SUM)

**INSTANCE:** Graph  $G = (V, E)$ .

**PROBLEM:** Find the enumeration scheme  $f : V \rightarrow \{1, 2, \dots, n\}$  that minimises the cost function

$$C(f) = \sum_{(\alpha, \beta) \in E} |f(\alpha) - f(\beta)|. \quad (21)$$

Figure 5 surveys the graphs with known solutions, as of the date of publication of Hortons's PhD thesis [27] which cites a solution for outerplanar graphs by Frederickson and Hambrusch [30]. Other sources include a survey by Lai [31], and solution for tree graphs by Chung [32]. This problem is known to be NP-complete via a reduction to the simple max-cut problem [22].

Finally, the last problem we consider is:

#### BANDWIDTH (or MINIMUM $\infty$ -SUM)

**INSTANCE:** Graph  $G = (V, E)$ .

**PROBLEM:** Find the enumeration scheme  $f : V \rightarrow \{1, 2, \dots, n\}$  that minimises the cost function

$$\max_{(\alpha, \beta) \in E} |f(\alpha) - f(\beta)|. \quad (22)$$

This is the minimum  $p$ -sum problem as  $p \rightarrow \infty$ . If  $G$  is an arbitrary tree graph, it is an NP-complete problem to solve the bandwidth problem for  $G$  [23]. In fact, Saxe proves that the decision

problem as to whether the bandwidth is less than or equal to  $k = O(1)$  is efficiently solvable [33].

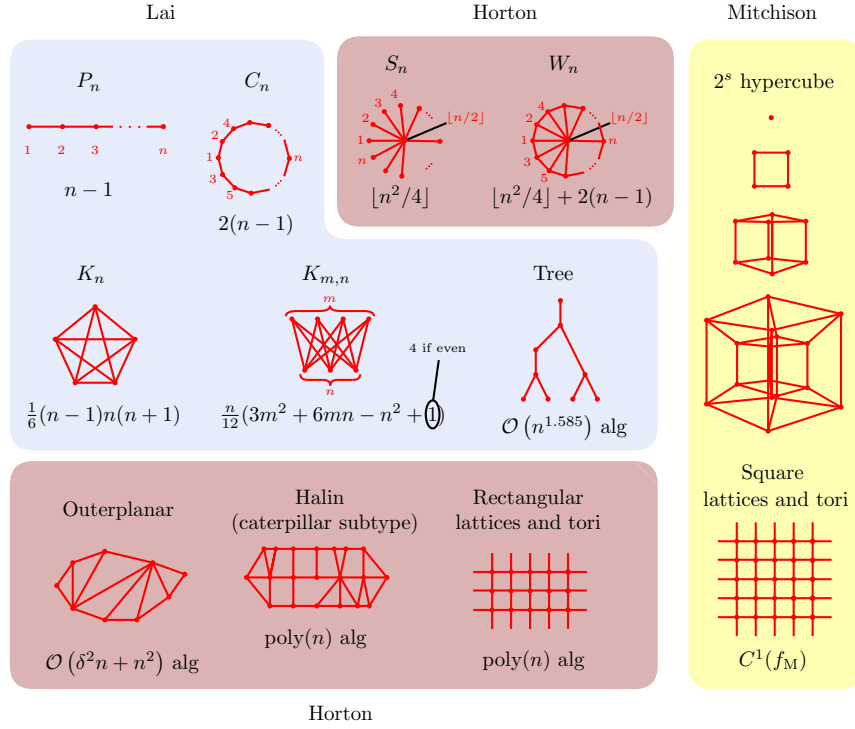


Figure 5: Graph families with known solutions to their edgesum problems. The formula for the minimum edgesum appears beneath each graph’s image, if it exists, or the cost of the best-known classical algorithm for solving that graph’s edgesum problem if not. References for the solution of these graphs appear in Lai [31], Horton [27], and Mitchison’s [21] works as indicated.

### 3 Fermion enumeration schemes and quantum circuit cost

In this section, we only consider Jordan-Wigner transformations from  $n$ -fermion to  $n$ -qubit systems. However, recent works such as the Verstraete-Cirac and Steudtner mappings [12, 16] use  $m > n$  qubits. We show how to incorporate our results into auxiliary qubit Jordan-Wigner mappings in Section 4.2.

#### 3.1 Enumeration schemes and figures of merit

Given an  $n$ -fermion system with a Hamiltonian  $H$ , the first step of any Jordan-Wigner process is always to label the fermions with an enumeration scheme. The Jordan-Wigner transform then maps the Hamiltonian’s hopping terms  $a_i^\dagger a_j$  to Pauli strings on the 1D qubit array. Any given enumeration scheme  $f$  thus generates a unique list of Pauli strings.

We propose the strategy of choosing fermion enumeration scheme that minimise the following properties of the induced list of Pauli strings. These properties pertain to the efficiency of the quantum computer, be it depth, gate count, or some other measure. We define several such key metrics below.

1. **Average Pauli weight.** The *Pauli weight* of a string of Pauli operations is the number of qubits involved in the string. A natural property to try and minimise by choosing an enumeration scheme  $f$  is the average weight of all the Pauli strings that the corresponding Jordan-Wigner transform produces. This corresponds to minimising the objective function

$$C^1(f) := \sum_{(i,j) \in f(G_F)} |i - j|, \quad (23)$$

where  $f(G_F)$  is the graph  $G_F$  with enumeration scheme  $f$  applied to its vertices. For a given fermion connectivity graph  $G_F$ , the formula for the average Pauli weight of enumeration  $f$  (denoted as  $APV(f)$ ) is

$$APV(f) := \frac{C^1(f)}{|G_F|} + 1, \quad (24)$$

where  $|G_F|$  is the number of edges in  $G_F$ . The extra term of 1 accounts for the fact that the weight of a Pauli string between qubits with labels  $i$  and  $j$  is  $|i - j| + 1$ . Figure 6 shows the average Pauli weight for enumeration schemes  $f_S$ ,  $f_Z$ ,  $f_M$  on the  $6 \times 6$  lattice.

The search for such an enumeration scheme is an example of the NP-complete problem known as Optimal Linear Arrangement problem. In Section 3.2, we present Theorem 1 for the enumeration scheme that minimises the average Pauli weight of a Jordan-Wigner mapping if  $G_F$  is the square lattice. Through Corollary 1.3, this lends an improvement to existing protocols for square lattice fermion simulation by reducing the average Pauli weight by up to  $\approx 13.9\%$ .

2. **Average  $p$ th power of Pauli weight.** One might want to optimize locality of the interactions which is quantified by the average  $p$ th power of the Pauli weights, where  $p \in \mathbb{R}^+$ . Minimising this property corresponds to finding the enumeration scheme  $f$  that minimises the objective function

$$C^p(f) := \left( \sum_{(i,j) \in f(G_F)} |i - j|^p \right)^{1/p}. \quad (25)$$

In Section 3.5, we present numerical results for the minimum- $p$ -sum problem to illustrate how one might choose fermion enumeration schemes to optimize over this objective function.

3. **Depth of circuit implementing of all Pauli strings.** In contrast to the above, another way to quantify the effectiveness of the enumeration scheme is the smallest number of timesteps in which a quantum circuit might implement all Pauli strings. Figure 7 shows quantum circuits implementing all hopping terms on the  $6 \times 6$  lattice for enumeration schemes  $f_S$ ,  $f_Z$ , and  $f_M$ , along with the depths of these circuits.

- 4. Other properties.** One may also consider other properties. For example, if the qubits have a connectivity graph  $G_Q$ , it may be desirable to make the Pauli strings as local as possible on  $G_Q$ . We include a discussion of this optimization in Section 4.2.

### 3.2 Minimising the average Pauli weight for a square fermionic lattice

We will now exhibit the optimal fermion-qubit mapping – the one which minimizes the average Pauli weight. It turns out that the most efficient way to label fermions is related to the work of Graeme Mitchison and Richard Durbin when they studied the organization of nerve cells in the brain cortex [21]. This pattern is dramatically different to the S-pattern and its variations [12, 16]. The pattern is depicted in the rightmost column of Figure 6 and in Figure 19. The proof of our main result below makes use of this curious arrangement to construct a spin fermionic mapping with optimal  $C^1(f)$  locality.

**Theorem 1.** (*Minimising the average Pauli weight of the Jordan-Wigner mapping for the  $n$ -fermion square lattice.*) Given a system of  $n = N^2$  fermions interacting in a square  $N \times N$  lattice  $G_F$ , then the Mitchison-Durbin pattern  $f_M$  is a fermion enumeration scheme that minimises the average Pauli weight of the hopping terms.

*Proof.* Proof in Section 3.3. □

**Corollary 1.1.** Optimizing the average Pauli weight depends on the edgesum value  $C^1(f)$ , therefore calculating the optimal fermion enumeration scheme for an arbitrary fermion graph  $G_F$  is NP-complete as discussed in Section 2.5.

Corollary 1.2 details all known scenarios to date where the optimal fermion enumeration scheme is solvable in  $\text{poly}(n)$  time.

**Corollary 1.2.** (*Solutions for other graph types  $G_F$ .*) If the Hamiltonian  $H$  is as defined in Theorem 1, and if  $G_F$  belongs to any of the graph families in Figure 5, then a classical computer can efficiently find an optimal fermion enumeration scheme for  $H$ .

*Proof.* Proof in Section 3.3. □

**Corollary 1.3.** Using the Mitchison-Durbin pattern  $f_M$  to enumerate a square-lattice fermionic system produces Pauli strings with an average weight of  $\frac{1}{3}(4 - \sqrt{2}) \approx 0.86$  times the corresponding average Pauli weight that the S-pattern  $f_S$  produces. That is, quantum circuits to implement the lattice hopping terms are shorter by 13.9%.

*Proof.* On an  $N \times N$  lattice, the Mitchison-Durbin pattern  $f_M$  and the S-pattern  $f_S$  have edgesums

$$C^1(f_S) = N^3 - N \tag{26}$$

$$C^1(f_M) = N^3 - xN^2 + 2x^2N - \frac{2}{3}x^3 + N^2 - xN - 2N + \frac{2}{3}x, \tag{27}$$

respectively. In Equation 27, the value  $x$  is the closest integer to  $N - \frac{1}{2}\sqrt{2N^2 - 2N + \frac{4}{3}}$  (proof in Section 3.3.1). By inspection,  $C^1(f_S) > C^1(f_M)$  for  $N \geq 6$ . With computer assistance it is straightforward to calculate the limit of the ratio of the two patterns' edgesums:

$$\lim_{N \rightarrow \infty} \frac{C^1(f_M)}{C^1(f_S)} = \frac{4 - \sqrt{2}}{3} \approx 0.86. \tag{28}$$

## Fermion enumeration scheme

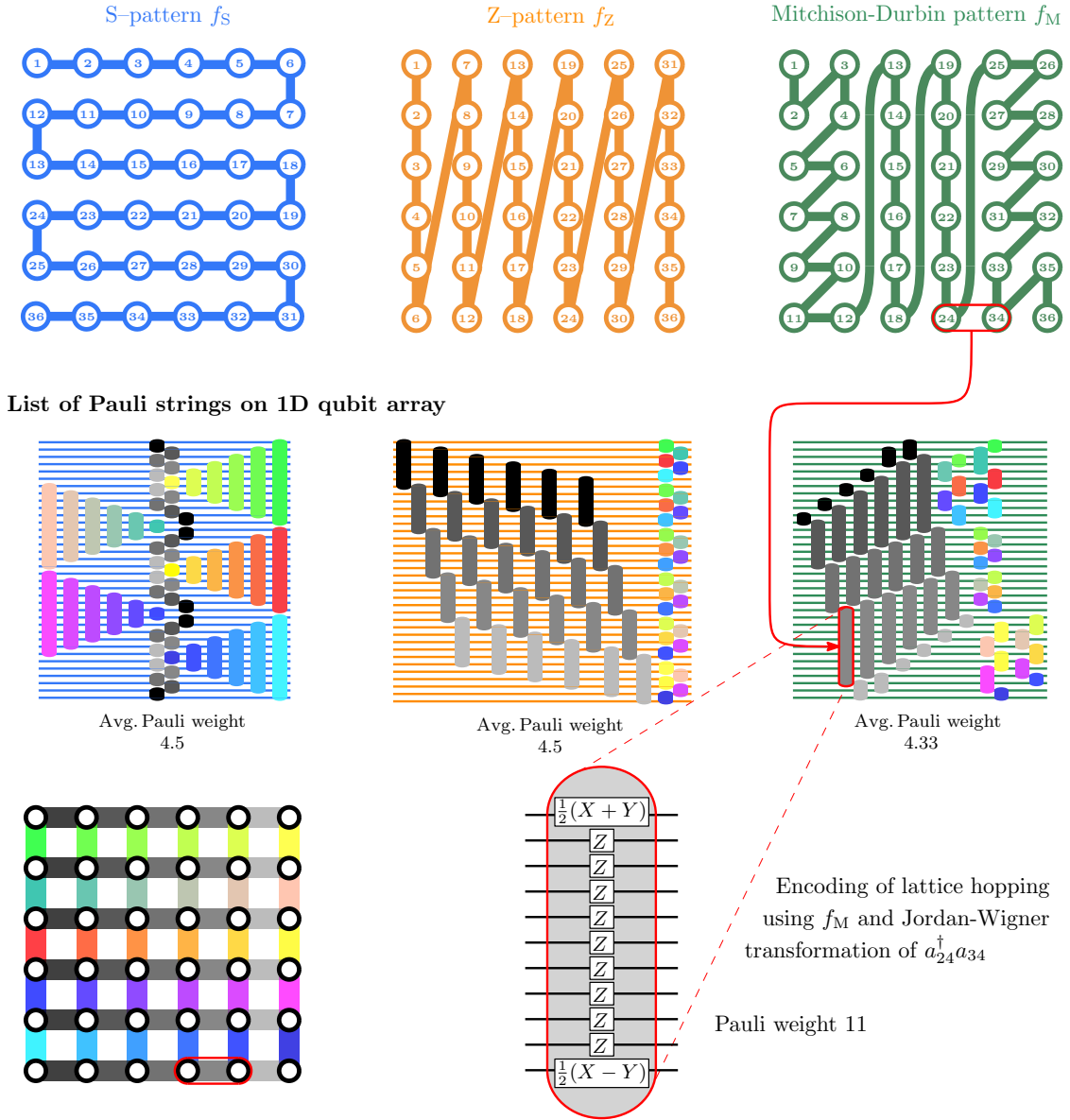


Figure 6: Three different enumeration schemes for the  $6 \times 6$  lattice of fermions and the Pauli strings they produce. Pauli strings correspond to the hopping term of the same colour in the  $6 \times 6$  lattice in the bottom left of the figure. On square lattices, the Mitchison-Durbin pattern produces Pauli strings of the lowest average weight.

Minimum depth of all Pauli strings

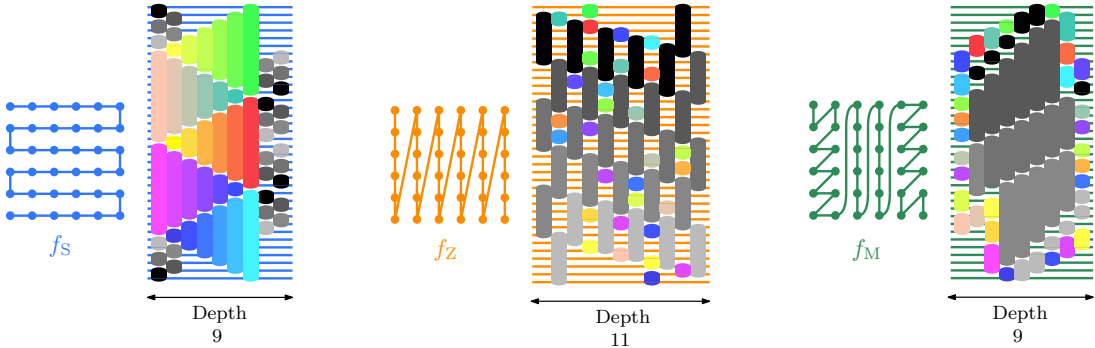


Figure 7: Comparison of the “parallelisability” of Pauli strings produced by three different enumeration schemes on a  $6 \times 6$  square lattice of fermions. The unit of merit is the depth of a quantum circuit implementing all Pauli strings. Pauli strings correspond to hopping terms of the same colour in the lattice in Figure 6.

In terms of the resource savings in designing a quantum computer, using Equation 24 the average Pauli weights approach the same limit:

$$\lim_{N \rightarrow \infty} \left( \left( \frac{C^1(f_M)}{2N(N-1)} + 1 \right) \left( \frac{C^1(f_S)}{2N(N-1)} + 1 \right)^{-1} \right) = \lim_{N \rightarrow \infty} \frac{C^1(f_M)}{C^1(f_S)} = \frac{4 - \sqrt{2}}{3} \approx 0.86. \quad (29)$$

□

We can conclude from Corollary 1.3 that a quantum computer simulation of a square fermionic Hamiltonian could save over 13.9% on quantum gate resources simply by labelling the fermions using the Mitchison-Durbin pattern rather than the S-pattern. Even in the case of simulating small fermionic systems, this method provides a worthwhile advantage. For example, in Figure 6 where  $N = 6$ , the ratio of the average Pauli weights using  $f_M$  and  $f_S$  is  $4.33/4.5 \approx 0.96$ . That is, even for the  $6 \times 6$  lattice, applying Theorem 1 could reduce quantum circuit size by 4%.

For  $2 \leq N \leq 20$ , Figure 8 shows the edgesums of various enumeration schemes on  $N \times N$  lattices. For  $N = 20$ ,  $C^1(f_M)/C^1(f_S) = \frac{7140}{7980} \approx 89.5\%$ . Even on lattices of these restricted sizes, the Mitchison-Durbin pattern can yield a reduction of over 10% from that of the S-pattern.

### 3.3 Proof of Theorem 1

The Mitchison-Durbin pattern  $f_M$  solves the Minimum-1-Sum problem for an  $N \times N$  lattice. Using this fact, it will become clear that the pattern  $f_M$  is an optimal choice to minimise the average Pauli weight of a Jordan-Wigner mapping, and Theorem 1 follows as a consequence. The structure of this section follows that of the original proof [21].

Let  $G = (V, E)$  be the  $N \times N$  square lattice. Label each vertex  $\alpha \in V$  by its position  $(\mu, \nu)$  on the lattice, where  $\mu, \nu \in \{1, 2, \dots, N\}$ . For example, the vertex in the top-left corner has label  $(1, 1)$  and the vertex in the bottom-right has label  $(N, N)$ .

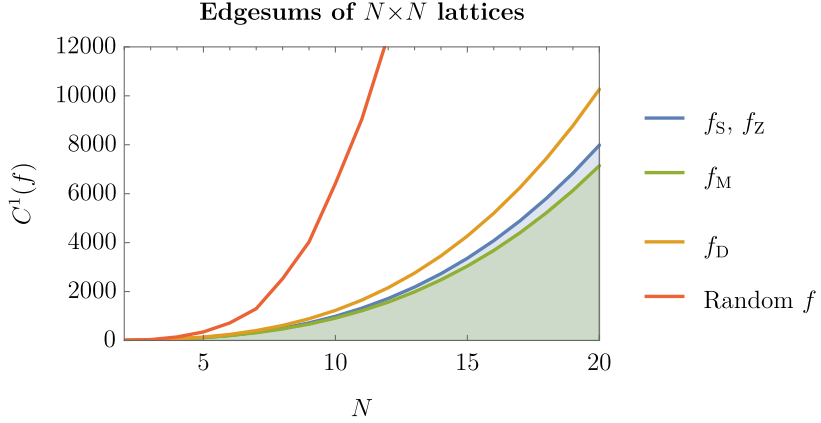


Figure 8: The edgesums  $C^1(f)$  of various enumeration schemes on  $N \times N$  lattices. Random  $f$  is a randomly-generated enumeration scheme in this instance.

Given a vertex enumeration scheme  $f : V \rightarrow \{1, 2, \dots, N^2\}$  for the lattice, the cost function for the minimum- $p$ -sum problem is then

$$(C^p(f))^p = \sum_{(\alpha, \beta) \in E} |f(\alpha) - f(\beta)|^p \quad (30)$$

$$= \sum_{(\mu, \nu) \in V} \left( \underbrace{|f(\mu+1, \nu) - f(\mu, \nu)|^p}_{\text{horizontal; 0 if } (\mu+1, \nu) \notin V} + \underbrace{|f(\mu, \nu+1) - f(\mu, \nu)|^p}_{\text{vertical; 0 if } (\mu, \nu+1) \notin V} \right). \quad (31)$$

Call an enumeration scheme  $f$  for the square lattice  $G$  *horizontally ordered* if  $f(\mu, \nu+1) > f(\mu, \nu)$  for all vertices  $(\mu, \nu) \in V$ . Similarly, call  $f$  *vertically ordered* if  $f(\mu+1, \nu) > f(\mu, \nu)$  for all  $(\mu, \nu) \in V$ .

**Proposition 1.** *Given a vertex enumeration scheme  $f : V \rightarrow \{1, 2, \dots, N^2\}$  for the  $N \times N$  square lattice, then there exists a horizontally and vertically ordered enumeration scheme  $g$  such that  $C^p(g) \leq C^p(f)$ . That is, there exists an optimal enumeration scheme for the  $N \times N$  square lattice that is horizontally and vertically ordered.*

*Proof.* Let  $f$  be a vertex enumeration scheme for the square lattice. Consider the enumeration scheme  $f'$  which is horizontally ordered, but otherwise the same as  $f$ . Thus, each row of the enumerated lattice  $f'(G)$  contains the same set of indices as  $f(G)$ , except that the indices are permuted so as to be in order of ascending value if they were not already. Call the process of replacing  $f$  with  $f'$  the *horizontal ordering of  $f$* . Define the *vertical ordering of  $f$*  similarly. Observe the following:

1. *The action of horizontally ordering  $f$  never increases  $C^p(f)$ .* Begin by proving the following:

Claim: The horizontal ordering of  $f$  will always decrease the horizontal contributions to  $C^p(f)$  in Equation 31 if  $p \geq 1$ .

Proof: Suppose  $f$  is not horizontally ordered; for example, there may be a row of the enumerated lattice  $f(G)$  such as the one in the top diagram of Figure 9. The horizontal contributions

to  $C^p(f)$  from this row are

$$|j_1 - j_2|^p + \cdots + |j_{i-1} - j_i|^p + |j_i - j_{i+1}|^p + \cdots + |j_{N-1} - j_N|^p. \quad (32)$$

Consider modifying  $f$  by rearranging the positions of  $j_{i+1}$  and  $j_i$ , as in the second diagram of Figure 9. The contributions to  $C^p(f)$  would now be:

$$|j_1 - j_2|^p + \cdots + |j_{i-1} - j_{i+1}|^p + |j_{i+1} - j_i|^p + \cdots + |j_{N-1} - j_N|^p. \quad (33)$$

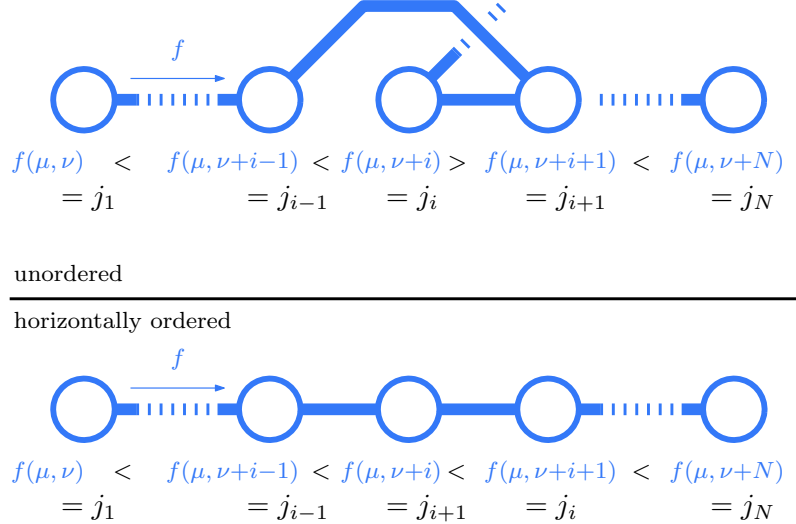


Figure 9: On a square lattice graph, horizontally ordering each row never increases the edgesum.

The difference in the horizontal contribution to  $C^p(f)$  upon modifying  $f$  in this way is thus the difference between Equations 33 and 32. This value is  $|j_{i-1} - j_{i+1}|^p - |j_{i-1} - j_i|^p < 0$  if  $p \geq 1$  because  $j_{i+1} < j_i$ .

The action of horizontally ordering  $f$  is simply a chain of as many swaps of the above form as is necessary to leave the vertices in each row of the lattice in ascending order. Thus, horizontally ordering  $f$  will always decrease the horizontal contributions to  $C^p(f)$  if  $p \geq 1$ . ■

Next, prove the following:

Claim: The horizontal ordering of  $f$  will never increase the vertical contributions to  $C^p(f)$  in Equation 31 if  $p \geq 1$ .

Proof: (Use Figure 10 as a guide.) Suppose that  $f$  is not horizontally ordered. Vertical contributions to  $C^p(f)$  will change upon the horizontal ordering of  $f$  if the process affects adjacent rows differently. This occurs if there exist vertices  $(\mu, \nu)$  and  $(\mu, \nu + 1)$  which are horizontally ordered with  $f(\mu, \nu) = i < f(\mu, \nu + 1) = j$ , and if vertices  $(\mu + 1, \nu)$  and  $(\mu + 1, \nu + 1)$  are not, with  $f(\mu + 1, \nu) = m > f(\mu + 1, \nu + 1) = n$ .

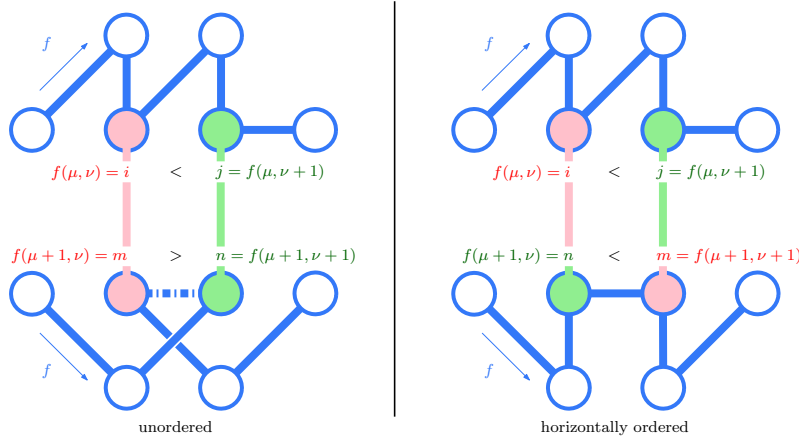


Figure 10: On a square lattice graph, the action of horizontally ordering a vertex enumeration scheme  $f$  never increases the vertical contributions to  $C^p(f)$ .

Initially, the vertical contributions to  $C^p(f)$  from these four vertices is

$$|i - m|^p + |j - n|^p. \quad (34)$$

Because  $i < j$  and  $m < n$ , the values  $(i - m)$  and  $(j - n)$  in 34 are unequal. Consider modifying  $f$  by rearranging the positions of  $m$  and  $n$ , as in Figure 10. The new vertical contributions are

$$|i - n|^p + |j - m|^p. \quad (35)$$

The values of  $(i - n)$  and  $(j - m)$  may not be equal, but they are closer in value to each other than the values  $(i - m)$  and  $(j - n)$  were. For  $p > 1$ , if  $a + b$  is constant then  $a^p + b^p$  reduces in value the closer  $a$  and  $b$  are to each other. Therefore, the vertical contributions to  $C^p(f)$  in Equation 35 are less than the vertical contributions in Equation 34. If  $p = 1$ , the contributions are unchanged by the modification. This proves the claim.  $\blacksquare$

These two claims show that the action of horizontally ordering  $f$  never increases  $C^p(f)$ .

2. *The action of vertically ordering a horizontally ordered enumeration scheme  $f$  preserves its horizontal ordering.* Suppose that  $f$  is a horizontally ordered enumeration scheme.

Claim: The vertical ordering of  $f$  preserves the horizontal ordering.

Proof: (Use Figure 11 as a guide.) Let  $g$  be the vertically ordered version of  $f$ , and suppose that it is not horizontally ordered. Then there must be a pair of vertices  $(\mu, \nu)$  and  $(\mu, \nu') \in V$  in the lattice such that  $g(\mu, \nu) = k < g(\mu, \nu')$  and  $\nu' < \nu$ , for  $k \in \{1, 2, \dots, N^2\}$ .

The enumeration scheme  $g$  is vertically ordered: therefore, each of the  $\mu - 1$  vertices above  $(\mu, \nu)$  must have a value less than  $g(\mu, \nu) = k$ . Because the vertex with label  $k$  is on the same row as  $(\mu', \nu)$ , then each of the  $\mu - 1$  vertices above  $(\mu, \nu')$  must also have a value less than  $k$ .

Now consider the original enumeration scheme  $f$ , before vertical ordering. The vertex with label  $k$  is in the same column of the lattice as it was under  $g$ , i.e. column  $\nu$ . Let this vertex be

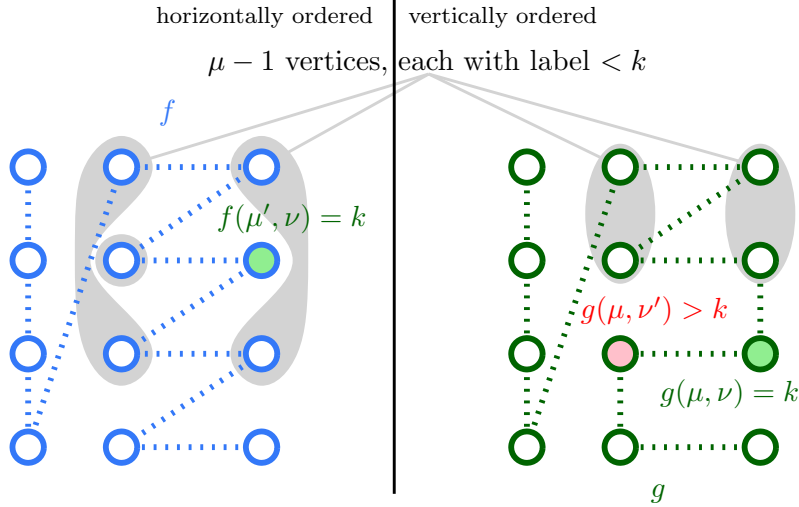


Figure 11: If a vertex enumeration scheme  $f$  is horizontally ordered, then its vertical ordering  $g$  must also be horizontally ordered. This figure shows the contradiction that would arise if this were not the case.

$(\mu', \nu)$ ; then  $f(\mu', \nu) = k$ . Because  $g$  is just a vertical ordering of  $f$ , there must still be  $\mu - 1$  vertices in columns  $\nu$  and  $\nu'$  with label less than  $k$ , and because  $f$  is horizontally ordered then every vertex to the left of these  $\mu - 1$  vertices has a label with value less than  $k$ . But every vertex to the left of  $(\mu', \nu)$  must also have a label with value less than  $k$ , as  $f(\mu', \nu) = k$ . Therefore, under the enumeration scheme  $f$ , any column to the left of column  $\nu$  contains  $(\mu - 1) + 1 = \mu$  vertices with labels of value less than  $k$ . But we know that column  $\nu'$  contains exactly  $\mu - 1$  vertices with label less than  $k$ , and  $\nu' < \nu$ . This is a contradiction. ■

3. For every vertex enumeration scheme  $f$  there exists a horizontally and vertically ordered scheme  $g$  with  $C^p(g) \leq C^p(f)$ . This is the result of combining the previous two statements.

This proves Proposition 1. □

Proposition 1 informs the discussion of numeric results when  $p > 1$  in Section 3.5. However, from this point the proof of Theorem 1 only concerns the minimum-1-sum problem, for which  $p = 1$ . Every enumeration scheme referenced from hereon is horizontally and vertically ordered. The following result greatly simplifies the calculation of  $C^1(f)$ :

Claim: Let  $V_l, V_r, V_t, V_b$  be the vertices in the left column, right column, top row and bottom row of the square lattice, respectively. Given a horizontally and vertically ordered vertex enumeration scheme  $f : V \rightarrow \{1, 2, \dots, N^2\}$  for the lattice, the cost function for the minimum-1-sum problem is

$$C^1(f) = \sum_{\alpha \in V_b} f(\alpha) + \sum_{\alpha \in V_r} f(\alpha) - \sum_{\alpha \in V_l} f(\alpha) - \sum_{\alpha \in V_t} f(\alpha). \quad (36)$$

Proof: As  $f$  is horizontally and vertically ordered, Equation 31 becomes

$$C^1(f) = \sum_{(\mu,\nu) \in V} \left( f(\mu+1, \nu) + f(\mu, \nu+1) - 2f(\mu, \nu) \right) \quad (37)$$

$$= 2f(N, N) + \sum_{\mu=2}^{N-1} f(\mu, N) + \sum_{\nu=2}^{N-1} f(N, \nu) - \sum_{\mu=2}^{N-1} f(\mu, 1) - \sum_{\nu=2}^{N-1} f(1, \nu) - 2f(1, 1) \quad (38)$$

$$= \sum_{\alpha \in V_b} f(\alpha) + \sum_{\alpha \in V_r} f(\alpha) - \sum_{\alpha \in V_l} f(\alpha) - \sum_{\alpha \in V_t} f(\alpha). \quad (39)$$

■

Any horizontally and vertically ordered enumeration scheme  $f$  must begin at a corner of the square lattice and end at the opposite corner. Assume without loss of generality that  $f(1, 1) = 1$  and  $f(N, N) = N^2$ , and that  $f(N, 1) < f(1, N)$ . As in Figure 12, let  $U$  be the section of the lattice that  $f$  labels up to  $(N, 1)$ , and let  $V$  be the section of the lattice that it labels from  $(N, 1)$  onwards. Because  $f$  can never “double back” on itself without violating horizontal or vertical ordering, the regions  $U$  and  $V$  are upper- and lower- skew block-triangular sections of the lattice, respectively.

Define  $S(U)$  and  $S(V)$  to be the sums of the labels of vertices on the boundary of the lattice in the regions  $U$  and  $V$ , respectively. By Equation 36, these  $S$  quantities completely determine the contributions to  $C^1(f)$  from the vertices in  $U$  and  $V$ . Suppose that  $U$  and  $V$  are fixed regions, and that the goal is to choose an enumeration scheme  $f$  to maximise  $S(U)$  and minimise  $S(V)$ . Lemma 2 provides a strategy to solve this problem.

**Lemma 2.** Let  $U$  and  $V$  be upper- and lower- skew block-triangular regions of the  $N \times N$  square lattice, containing vertices  $(N, 1)$  and  $(1, N)$  respectively, as above. For any enumeration scheme  $f : V \rightarrow \{1, 2, \dots, N^2\}$  that labels the vertices in  $U$  before any outside of  $U$ , and labels the vertices in  $V$  after any outside of  $V$ , define  $S(U)$  and  $S(V)$  to be the sums of the labels on the lattice boundaries of  $U$  and  $V$ , respectively. Then, the rules below construct a horizontally and vertically ordered enumeration scheme  $f$  that yields the maximum value for  $S(U)$ :

- Fill each new column/row as far as possible while preserving horizontal and vertical ordering;
- After filling a column/row as far as possible, begin to fill the longest remaining column/row that remains, starting from the top-leftmost available vertex of the lattice.

By symmetry, the reverse of this process provides a scheme that yields the minimum value for  $S(V)$ .

*Proof.* (For reference, Figure 12 provides one example each of ordered enumeration schemes that do and do not satisfy the rules in Lemma 2.)

For a): if  $f$  did not fill a row as far as possible, then the first label on the subsequent column would be less than if  $f$  had filled the initial row, as Figure 13 demonstrates. Only the first entries of each row and column contributing to  $S(U)$ , so this is not an optimal result.

For b): suppose that, beginning at index  $i$ , the enumeration scheme  $f$  fills a column of length  $x$  before it fills a row of length  $y > x$ , as in Figure 14. Then the contribution of the row and column to  $S(U)$  is  $i + (i + x)$ . However, following rule b) in Lemma 2 would mean filling the row before the column, and the contribution to  $S(U)$  would be  $i + (i + y) > i + (i + x)$ . Therefore, optimal enumeration schemes must follow rule b) as well as rule a).

Note that rules a) and b) describe a unique enumeration scheme for  $U$ , and so it is not possible to prescribe any further rules. Thus the resulting enumeration scheme must maximise  $S(U)$ . □

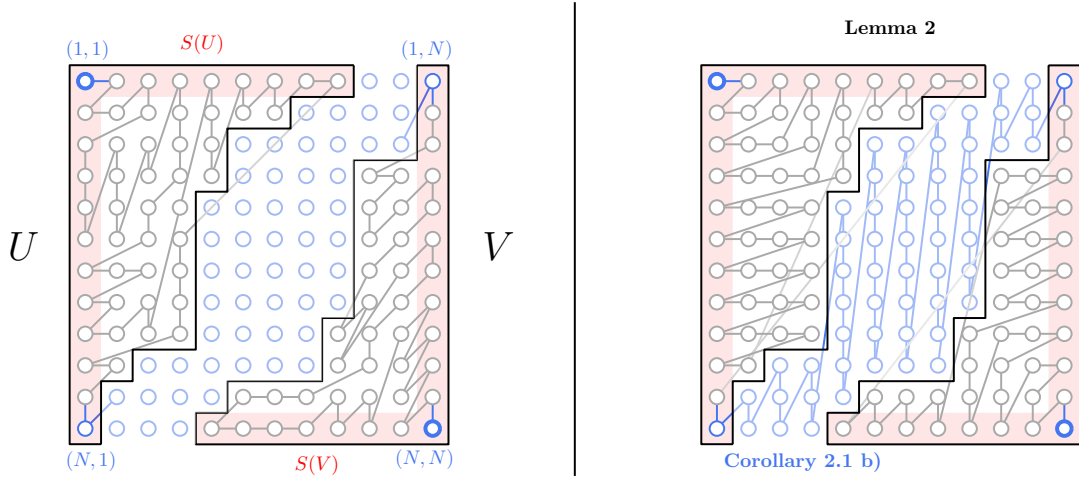


Figure 12: **Left:** An example of the regions  $U$  and  $V$ , and an ordered enumeration scheme that does not follow the rules in Lemma 2. Vertices on the boundaries of  $U$  and  $V$  contribute to  $S(U)$  and  $S(V)$ . **Right:** An example of an enumeration scheme that follows the rules in Lemma 2 and hence maximises  $S(U)$  and minimises  $S(V)$ . The scheme fills the space between  $U$  and  $V$  with vertical columns as a consequence, via Corollary 2.1 b).

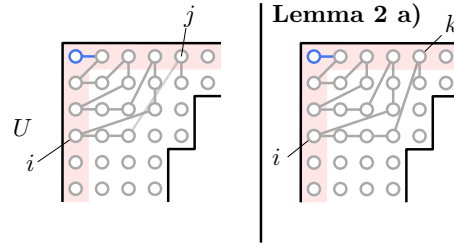


Figure 13: **Left:** An enumeration scheme that does not fill the row containing label  $i$  as far as possible. **Right:** The enumeration scheme now fills the row containing  $i$  as far as possible whilst preserving horizontal and vertical ordering. It is clear that  $k > j$ .

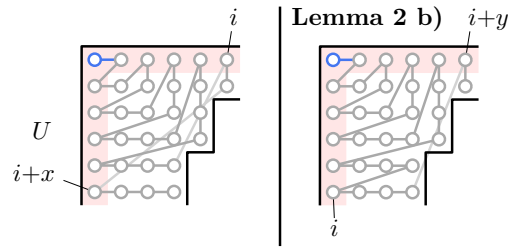


Figure 14: **Left:** An enumeration scheme that does not fill rows and columns in order of decreasing length. **Right:** The enumeration scheme now fills the row of length  $y$  before the column of length  $x < y$ . It is clear that  $i + (i + y) > i + (i + x)$ .

**Corollary 2.1.** The consequence of the rules in Lemma 2 is that an enumeration scheme  $f$  that minimises  $C^1(f)$  must:

- Fill the largest square that lies in  $U$  by alternating between successively longer rows and columns, before filling the remaining columns and rows of  $U$  that are outside the square in order of decreasing length (a detail that the rightmost diagrams in Figures 12 and 14 include);
- Fill  $\overline{U \cap V}$ , the region between  $U$  and  $V$ , with columns from top-to-bottom. This ensures that labels with the least possible value occupy the bottom row of the lattice outside  $V$ , and that labels with the greatest possible value occupy the top row of the lattice outside  $U$ .

Proof: Given Lemma 2, Corollary 2.1 is self-evident. Figure 12 illustrates Corollary 2.1 b).  $\blacksquare$

Lemma 2 showed how to minimise  $C(f)$  for fixed shapes of the regions  $U$  and  $V$ ; Lemmas 3 and 4 will show which shapes for  $U$  and  $V$  can give a global minimum for  $C^1(f)$ .

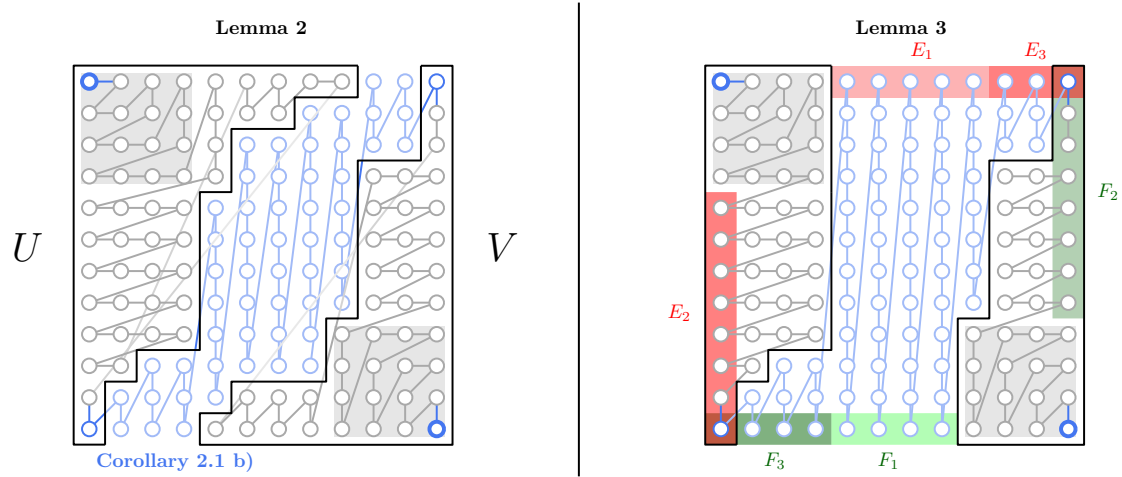


Figure 15: Lemma 3 shows how to delete regions of  $U$  and  $V$  so that the new enumeration scheme has a smaller edgesum  $C^1$ .

**Lemma 3.** Let  $U$  and  $V$  be regions of the  $N \times N$  square lattice that satisfy Lemma 2's conditions, and let  $f$  be an optimal enumeration scheme that follows the rules of Lemma 2. Then, delete from  $U$  the region to the right of the largest square in  $U$ , and add it to  $\overline{U \cap V}$ . Similarly, delete from  $V$  the region to the left of the largest square in  $V$ , and add it to  $\overline{U \cap V}$ . This reduces  $C^1(f)$ .

*Proof.* Define  $E_1$  to be sum of the labels of the topmost vertices in  $U$  that are to the right of the largest square in  $U$ ,  $E_2$  to be the sum of the labels of the leftmost vertices beneath the largest square in  $U$ , and  $E_3$  to be the sum of the labels of the topmost vertices outside of  $U$ . Define  $F_1$ ,  $F_2$  and  $F_3$  analogously, as in Figure 15. Then,

$$C^1(f) = (F_1 + F_2 + F_3) - (E_1 + E_2 + E_3) + \text{labels of edge vertices in squares}. \quad (40)$$

Any horizontally and vertically ordered enumeration scheme that follows the rules of Lemma 2 must label the vertices in the largest squares of  $U$  and  $V$  first and last. Therefore, the deletion operation in Lemma 3's statement does not change the labels of the edge vertices in the squares.

Claim: The deletion operation in Lemma 3 increases  $(E_1 + E_2 + E_3)$ .

Proof: The following three steps implement the deletion operation in Lemma 3.

1. Delete from  $V$  the region to the left of the largest square in  $V$ , and add it to  $\overline{U \cap V}$ . This increases  $E_3$  and leaves  $E_1$  and  $E_2$  unchanged.
2. Delete the rightmost column from  $U$ , and add it to  $\overline{U \cap V}$ . As in Figure 16, let  $x$  be the side length of the largest square in  $U$ , let  $w$  be the height of the rightmost column of  $U$  and let  $h$  be the height of the bottommost row of  $U$  with length greater than  $w$ . This step reduces the labels of the bottommost  $h$  elements in  $E_2$  by  $w$ , and so  $E_2$  decreases by  $hw$ . Meanwhile, the value of  $E_1$  increases because of the new label for the topmost vertex of the column that has joined  $\overline{U \cap V}$ . The label of this vertex increases by at least  $hx$ , and so the value of  $E_1 + E_2$  increases by  $hx - hw = h(x - w) > 0$ , as  $x > w$ .

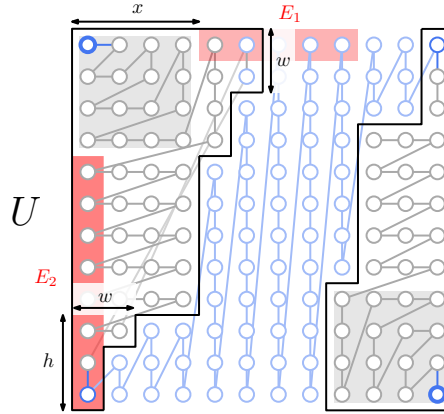


Figure 16: Deleting the rightmost column of  $U$  increases the value of  $E_1 + E_2$ .

3. Repeat step 2 until the entire region in  $U$  to the right of the largest square in  $U$  has joined  $\overline{U \cap V}$ . Breaking down the deletion operation in this way reveals that  $E_1 + E_2 + E_3$  increases. ■

By symmetry, the deletion operation must therefore decrease  $F_1 + F_2 + F_3$ , and so  $C^1(f)$  decreases overall. □

Finally, Lemma 5 shows how to structure the regions outside the largest squares in  $U$  and  $V$  to give the least value for  $C^1(f)$ .

**Lemma 4.** Let  $U$  and  $V$  be regions of the  $N \times N$  square lattice that satisfy Lemma 3's conditions, and let  $f$  be an optimal enumeration scheme that follows the rules of Lemma 2. Suppose the side length of the largest square in  $U$  is  $x$ . Then, modify  $U$  by imposing a length of  $x$  on all rows down to a height  $x$  above the bottom row, and then give the row at height  $y < x$  a length of  $y$  or  $y - 1$ . Perform the inverse modification to  $V$ .

The resulting optimal enumeration scheme with these new  $U$  and  $V$  yields the minimum  $C^1(f)$  over all possible enumeration schemes for the square lattice.

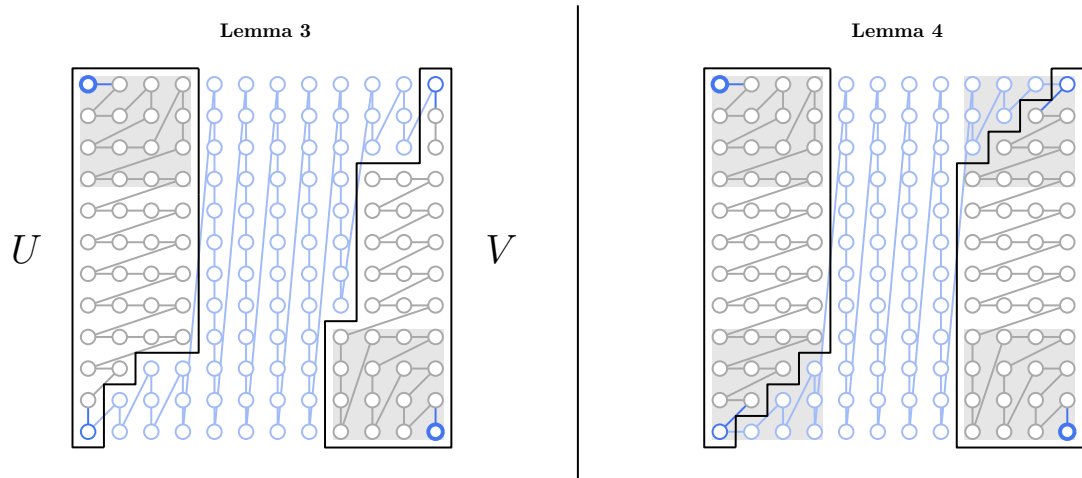


Figure 17: Lemma 4 shows the optimal shape for regions  $U$  and  $V$  in order to minimise the edgesum  $C^1$ . The resulting pattern is the Mitchison-Durbin pattern  $f_M$ .

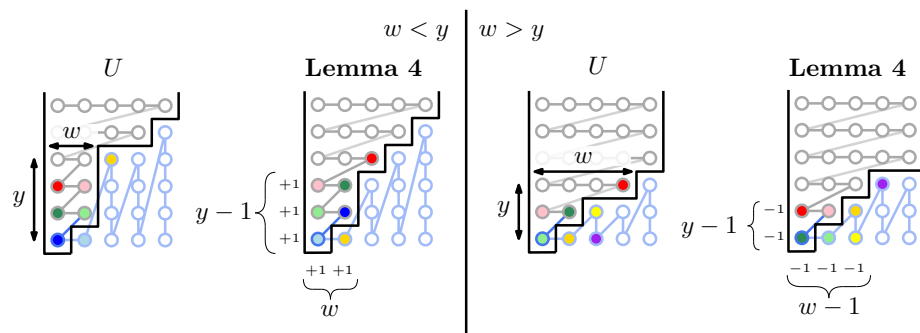


Figure 18: Modifying the shape of  $U$  in Lemma 4 to reduce the edgesum  $C^1$ .

*Proof.* As in Figure 18, take a row of  $U$  outside of the top-left square. Let it be the  $y$ th row from the bottom, and let its length be  $w$ . Then, if  $w < y$ , increase the row's length to  $w + 1$ . This increases by  $+1$  the labels of the  $y - 1$  bottommost vertices in the left-hand column of the lattice. Similarly, the labels of the  $w$  leftmost vertices in the bottom row increase by  $+1$ . With this modification to the enumeration scheme  $f$ , the value of  $C^1(f)$  changes by  $w - (y - 1) \leq 0$ , i.e. it decreases by  $(y - 1) - w \geq 0$ .

If  $w > y$ , decrease the row's length to  $w - 1$ . This subtracts  $1$  from the labels of the  $y - 1$  bottommost vertices in the left-hand column of the lattice, and from the labels of the  $w - 1$  leftmost vertices in the bottom row. Thus the value of  $C^1(f)$  changes by  $-(w - 1) - (y - 1) \leq 0$ , i.e. it decreases by  $w - y \geq 0$ .

By symmetry, the inverse process works on  $V$ . Repeated application of these steps thus minimises  $C^1(f)$ ; Figure 17 shows the end result.  $\square$

Only one degree of freedom remains in choosing the shape of  $U$ : the side length  $x$  of its largest square. Lemma 5 expresses the edgesum of the pattern as a function of  $N$  and  $x$ . Corollary 5.1 then provides the optimal value for  $x$  and hence the Mitchison-Durbin pattern  $f_M$ .

**Lemma 5.** Let  $U$  and  $V$  be regions of the  $N \times N$  square lattice that satisfy Lemma 4's conditions, and let  $f$  be an optimal enumeration scheme that follows the rules of Lemma 2. Suppose that the side lengths of the largest squares in  $U$  and  $V$  are both  $x$ . Then the edgesum of  $f$  is

$$C^1(f) = N^3 - xN^2 + 2x^2N - \frac{2}{3}x^3 + N^2 - xN - 2N + \frac{2}{3}x. \quad (41)$$

*Proof.* See Section 3.3.1.  $\square$

**Corollary 5.1.** For  $N \geq 5$ , the value of  $x$  that minimises  $C^1(f)$  in Equation 41 is  $x = N - \frac{1}{2}\sqrt{2N^2 - 2N + \frac{4}{3}}$ . Round  $x$  to the nearest integer to obtain the minimum  $C^1(f)$  over all enumeration schemes for the  $N \times N$  square lattice.

*Proof.* Treat  $N$  and  $x$  as continuous variables, and use calculus to find that minimum of  $C^1(f)$  in Equation 41 occurs when  $x = N - \frac{1}{2}\sqrt{2N^2 - 2N + \frac{4}{3}}$ .  $\square$

Note that the optimal value for  $x$  in Corollary 5.1 is a refinement on the value that Mitchison and Durbin give in [21]: they use the approximation  $x = \left(1 - \frac{1}{\sqrt{2}}\right)N$ . For all intents and purposes, these values are extremely close and rounding this approximate value for  $x$  gives the same integer as  $N - \frac{1}{2}\sqrt{2N^2 - 2N + \frac{4}{3}}$  for most values of  $N$ .

Define the Mitchison-Durbin pattern  $f_M$  to be any of the optimal enumeration schemes that fill region  $U$  first and region  $V$  last, where the value of  $N$  completely determines  $U$  and  $V$  via the successive restrictions of Lemmas 2–5 and Corollary 5.1. For example, in Figure 6,  $N = 6$  and  $x = 2$ . In Figure 19,  $N = 17$  and  $x = 5$ . This completes the proof.

### 3.3.1 Edgesum of the Mitchison-Durbin pattern

This section calculates the edgesum of the enumeration pattern  $f$  in Lemma 5. Divide the enumeration pattern on the  $N \times N$  grid up into regions  $A, B, \dots, G$  as in Figure 19. Let the label of each

region also denote its edgesum. Therefore

$$\begin{aligned} C^1(f) = & A + B + C + D + E + F + G \\ & + AB + AD + BD + BC + CD + DE + EF + DF + FG + DG, \end{aligned} \quad (42)$$

where  $AB, \dots, DG$  denote the sums of the differences between vertex labels across the interfaces between each pair of regions. Due to the symmetry of  $f$ , Equation 42 becomes

$$C^1(f) = 2(A + B + C) + D + 2(AB + AD + BC + BD + CD). \quad (43)$$

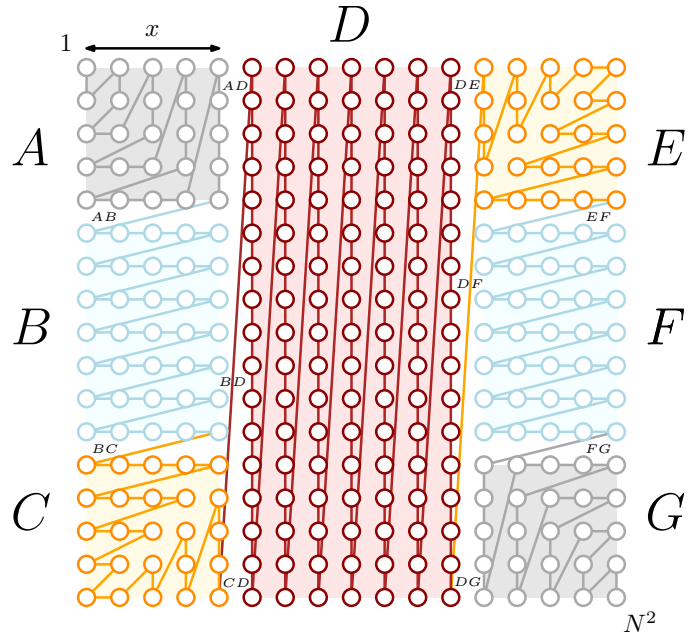


Figure 19: Sections of the  $N \times N$  square lattice and an enumeration pattern  $f$  that satisfies Lemma 4.

We can derive expressions for the contributions of each region to  $C^1(f)$  by observing the patterns in the differences between vertex labels. Figure 20 shows the progression of vertex labels in regions  $A$ – $D$  of the square lattice. Within each of these regions, the enumeration scheme is horizontally and vertically ordered. Thus, using Equation 36 on region  $A$  gives:

$$A = \left( \sum_{k=0}^{x-2} (x(x-2) + 2 + k) + \sum_{j=1}^x (x(x-1) + j) \right) - \left( \sum_{k=1}^x (k(k-1) + 1) + \sum_{j=1}^x (j(j-2) + 2) \right) \quad (44)$$

$$= \frac{1}{6}(x-1)(6 + x(8x-1)). \quad (45)$$

The other regions contribute the following quantities:

$$B = (N - 2x)(x - 1) + x^2(N - 2x - 1) \quad (46)$$

$$C = \frac{1}{6}(x - 1)(6 + x(8x - 1)) \quad (47)$$

$$D = N^3 - 2xN^2 - 2xN + 2x - N. \quad (48)$$

The vertex labels in Figure 20 also make it simple to calculate the contributions to  $C^1(f)$  from the interfaces between the regions:

$$AD = \sum_{j=1}^x \left( (x(x - 1) + j) - (Nx + j) \right) = Nx^2 - x^3 + x^2 \quad (49)$$

$$AB = 1 - 2x + 2x^2 \quad (50)$$

$$BD = \frac{1}{2} (N^2 + N - 3xN + xN^2 + 2x^2 - 2x - 2x^2N) \quad (51)$$

$$BC = x^2 \quad (52)$$

$$CD = 1 - 2x + xN + x^2. \quad (53)$$

Substituting Equations 45–53 into Equation 43 gives the result,

$$C^1(f) = N^3 - xN^2 + 2x^2N - \frac{2}{3}x^3 + N^2 - xN - 2N + \frac{2}{3}x. \quad (54)$$

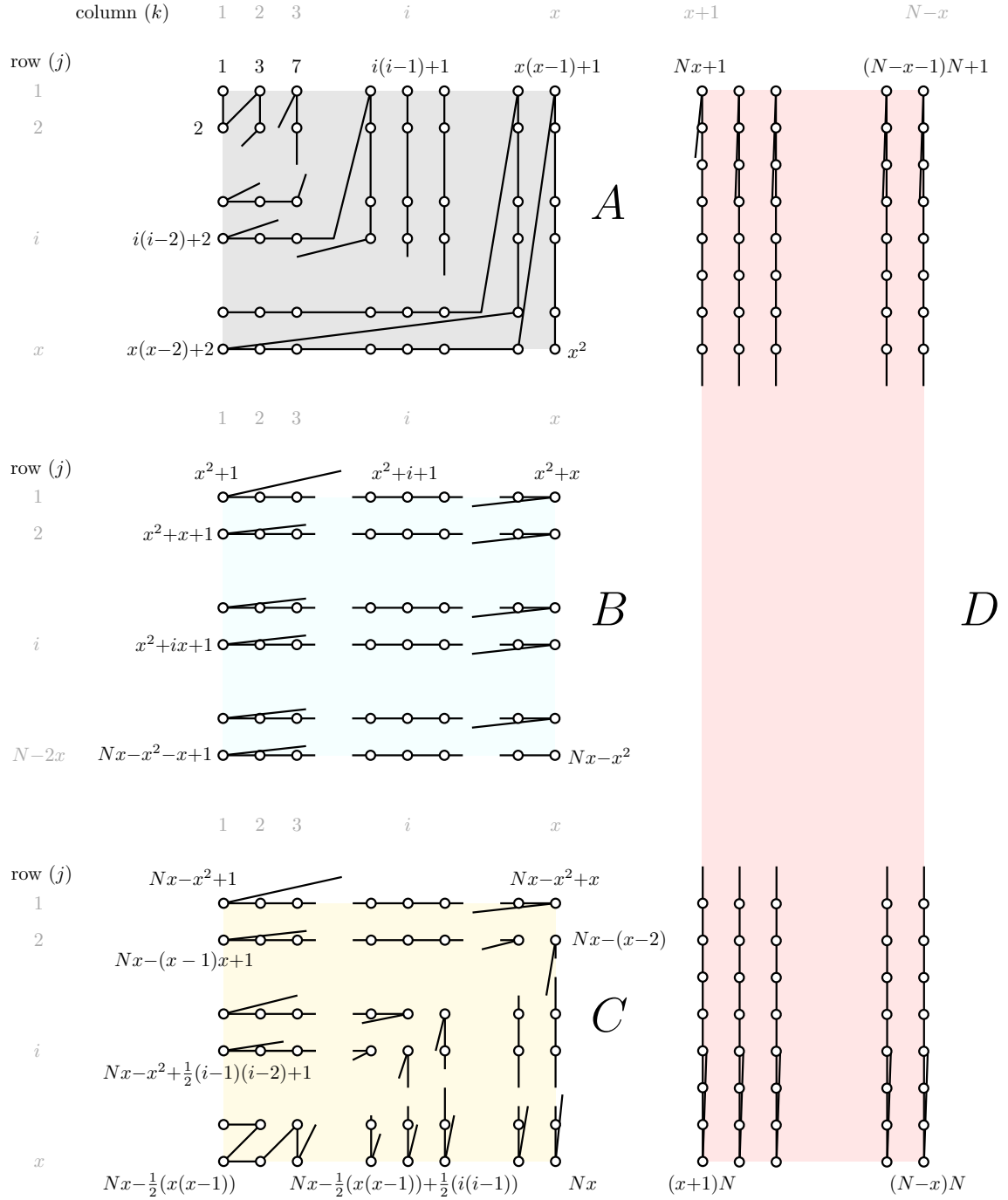


Figure 20: An in-depth look at the Mitchison-Durbin pattern  $f_M$ . Vertex labels indicate the position of each vertex in the enumeration scheme.

### 3.4 Reducing the average Pauli weight for cellular fermion graphs

Theorem 1 reduces the average gate count of fermionic Hamiltonian simulation on a square lattice by making judicious use of the solutions to the Edgesum problem. As Corollary 1.2 discusses, there are only a handful of other graph families for which there are known edgesum solutions. It might be tempting to think that there is not much use in trying to reduce average gate count via fermion enumeration scheme if the fermionic graph  $G_F$  does not belong to one of these families. In this section, however, we show an example graph for which a “common-sense” approach to constructing a good enumeration scheme can provide an order-of-magnitude reduction in average gate count.

Consider  $(n \times n) \times (N \times N)$  *cellular arrangements* of square fermionic lattices, where each  $n \times n$  sub-lattice of fermions connects to adjacent sub-lattices via a single edge. Here we use the cellular pattern in Figure 21, where the connections are from each  $n \times n$  lattice’s top left vertex to the two closest vertices from neighbouring lattices.

It is possible to enumerate the fermions on a cellular arrangement graph with the Z-pattern  $f_Z$  or the S-pattern  $f_S$  from Section 3.2, treating the whole graph as a single square lattice. As Figure 21 shows, another way of enumerating the fermions is to number each sub-lattice before moving on to the next, progressing through the entire graph via an S- or Z-pattern. We call these two enumeration procedures  $f_{S'}$  and  $f_{Z'}$ , respectively.

The edgesums of these enumeration schemes on the cellular arrangement graph are:

$$C^1(f_S) = \begin{cases} (Nn)^3 - Nn - N(N-1)(n-1) - \sum_{k=0}^{N-1} \sum_{i=kn+2}^{(k+1)n} (2i-1), & n \text{ even} \\ (Nn)^3 - Nn - N(N-1)(n-1) - \sum_{k=0}^{N-1} \sum_{i=kn+1}^{(k+1)n-1} (2i-1), & n \text{ odd}, \end{cases} \quad (55)$$

$$C^1(f_Z) = (Nn)^3 - Nn - N(N-1)(n-1) - nN^2(n-1)(N-1), \quad (56)$$

$$C^1(f_{Z'}) = \begin{cases} N^3n^2 + n^3N^2 - n^2N^2 - 2nN^2 - n^2N + 2N^2 + 2nN + n^2 - 2N - n, & n \text{ even} \\ N^3n^2 + n^3N^2 - n^2N^2 - nN^2 - n^2N + N^2 + 2nN + n^2 - 2N - 2n + 1, & n \text{ odd}, \end{cases} \quad (57)$$

$$C^1(f_{S'}) > C^1(f_{Z'}) \text{ and depends on parities of } n \text{ and } N. \quad (58)$$

By using  $f_{Z'}$  rather than  $f_Z$ , the edgesum of a large cellular arrangement graph reduces by an order of magnitude:

$$\lim_{N \rightarrow \infty} \frac{C^1(f_{Z'})}{C^1(f_Z)} = \frac{n^2}{n^3 - n^2 + n} = \mathcal{O}\left(\frac{1}{n}\right); \quad (59)$$

$$\lim_{n \rightarrow \infty} \frac{C^1(f_{Z'})}{C^1(f_Z)} = \frac{1}{N}. \quad (60)$$

If  $n = \mathcal{O}(N)$ , then the graph has  $\mathcal{O}(N^4)$  vertices. From choosing  $f_{Z'}$  rather than  $f_Z$ , the  $\mathcal{O}(1/N)$  factor reduction in edgesum is thus proportional to the fourth root of the number of vertices. This is a much more striking improvement than the constant-factor improvement that Corollary 1.3 proffers, even though we have not proved that  $f_{Z'}$  is an optimal enumeration scheme for the cellular arrangement graph.

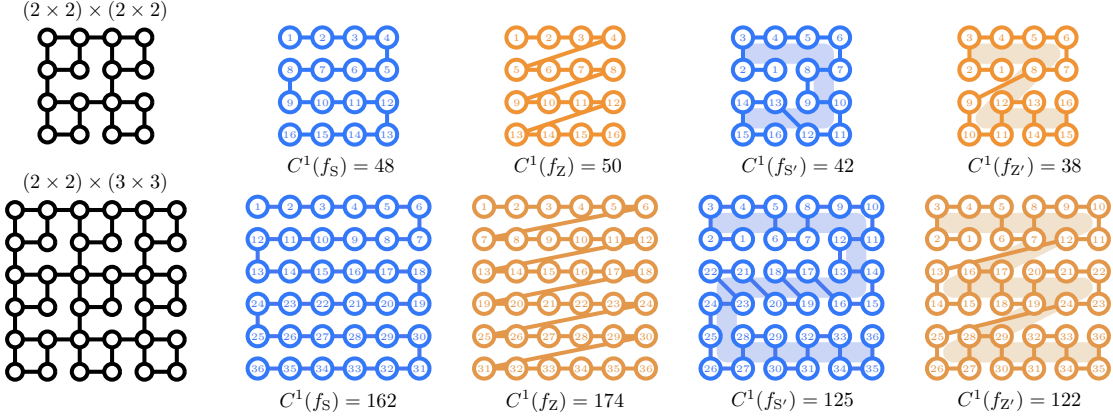


Figure 21: Edgesums for some enumeration schemes of  $(n \times n) \times (N \times N)$  cellular arrangement patterns.

### 3.5 Reducing the average $p$ th power of Pauli weight for a square lattice

In Section 3.1, we introduced other figures of merit for fermion enumeration schemes, such as the average  $p$ th power of Pauli weight for  $p > 1$ . For a given fermion graph  $G_F$ , this corresponds to finding the enumeration scheme  $f$  that minimises the  $p$ -sum

$$C^p(f) = \left( \sum_{(u,v) \in E} |f(u) - f(v)|^p \right)^{1/p}. \quad (61)$$

The  $p = 1$  case is the edgesum problem and via Corollary 1.1 is NP-complete. George and Pothen showed that the minimum 2-sum problem is also NP-complete [29]. They approach the minimum 1-sum and 2-sum problems for *any* graph  $G_F$  and develop spectral approaches to solving the minimum 1-sum and 2-sum problems. Separately, Mitchison and Durbin [21] explore the Minimum  $p$ -sum problem where the graph  $G$  is a square lattice, and conclude with Proposition 2:

**Proposition 2.** (Mitchison and Durbin's results for the minimum  $p$ -sum problem on an  $N \times N$  lattice [21]) *Given a system of  $n = N^2$  fermions interacting in a square  $N \times N$  lattice  $G_F$ , the following are the lower limits for the value of  $C^p(f)$ :*

- (a) *If  $0 < p < \frac{1}{2}$ , then there exists an enumeration scheme  $f$  with  $C^p(f) = \mathcal{O}(N^2)$ .*
- (b) *If  $\frac{1}{2} < p < 1$ , then  $C^p(f) \geq \frac{1}{2p+1} N^{1+2p} + \mathcal{O}(N^{2p})$ .*
- (c) *If  $p = 1$ , then  $f_M$  gives the minimum value as shown in Theorem 1.*
- (d) *If  $p > 1$ , then  $C^p(f) \geq \frac{4}{2^p(p+2)} N^{p+2}$ .*

The lower bounds in (b) and (d) are theoretical limits, and to date there are no known enumeration schemes that achieve their low coefficients. However, the “diagonal pattern”  $f_D$  has edgesum

$$C(f_D) \approx \frac{4}{p+2} N^{p+2} + \mathcal{O}(N^{p+1}), \quad (62)$$

which has the same order of magnitude in  $N$  as the theoretical limit in (d).

*Proof.* See Propositions 2–4 of [21].  $\square$

Below, we provide a table of known results and introduce several other simple enumeration patterns in the regime  $p \rightarrow \infty$ , where  $N \rightarrow \infty$ , and show the performance of the diagonal pattern in the  $p > 1$  regime. The diagonal pattern is the solution to the bandwidth problem on rectangles – in [21].

### 3.5.1 Performance of four enumeration schemes for $p \geq 1$

Lemma 6 takes the results of Proposition 2 (d) and illustrates the performance of four enumeration schemes:  $f_S$ ,  $f_M$ ,  $f_Z$ , and  $f_D$  (the S-, Mitchison-Durbin, Z- and diagonal patterns).

**Lemma 6.** (Best known results for the minimum  $p$ -sum problem on a square lattice) As summarised in Figure 22.

Enumeration scheme $f$	$C^1(f)$	$C^p(f)$ , $p > 1$
Mitchison-Durbin pattern $f_M$	$N^3 - xN^2 + 2x^2N - 2x^3/3 + N^2 - xN - 2N + 2x/3$	Includes terms $\geq \sim 2x^{p+1}N^p \sim 2k^{p+1}N^{2p+1}$ where $x = kN$
S-pattern $f_S$	$N^3 - N$	$(N-1) \left( \sum_{k=1}^{N-1} (2k+1)^p + N+1 \right) \sim \frac{2^p}{p+1} N^{p+2} + \mathcal{O}(N^{p+1})$
Z-pattern $f_Z$	$N^3 - N$	$(N-1)(N^{1+p} + N) = N^{p+2} - N^{p+1} + N^2 - N$
Diagonal pattern $f_D$	$4N^3/3 - N^2 - N/3$	$2 \left( \sum_{k=1}^{N-2} (2k+1)(k+1)^p + (N-1)N^p + 1 \right) \sim \frac{4}{2+p} N^{p+2} + \mathcal{O}(N^{p+1})$
Theoretical limit $\sim \frac{1}{2^p(2+p)} N^{p+2} + \text{smaller...}$		

Figure 22: Results for the minimum  $p$ -sum problem for the square lattice for  $p \geq 1$ . While the Mitchison-Durbin pattern  $f_M$  minimises  $C^p(f)$  for  $p = 1$ , it performs the worst of all the options for  $p > 1$ . The diagonal pattern  $f_D$  performs better than the rest for  $p > 2$ .

## 4 Discussion

We provide novel ways of improving on the fermion-qubit mappings by optimizing the fermion enumeration schemes; this provides the optimal result in the case of fermionic lattices, as Theorem 1 demonstrates. This technique is remarkably general and improve on Jordan-Wigner like mappings. In the following subsection we discuss our result in the context of existing techniques that work with fermionic hamiltonians. This is followed by Section 4.2 where we show how our approach can boost the effectiveness of other state-of-the-art approaches to mapping between fermions and qubits. In Section 4.3 we suggest an approach to hybridising our fermion enumeration scheme strategy with a constant number of auxiliary qubits to further increase the locality of Hamiltonians.

### 4.1 Fermion enumeration schemes in the context of quantum simulation

This section illustrates the context within which our result provides immediate practical value: the reduction of gate count in quantum algorithms for solving generic instances of quantum chemistry problems and beyond. Figure 23 offers a top-down summary of the state of the field and the precise place our techniques occupy in the context of simulating physical systems.

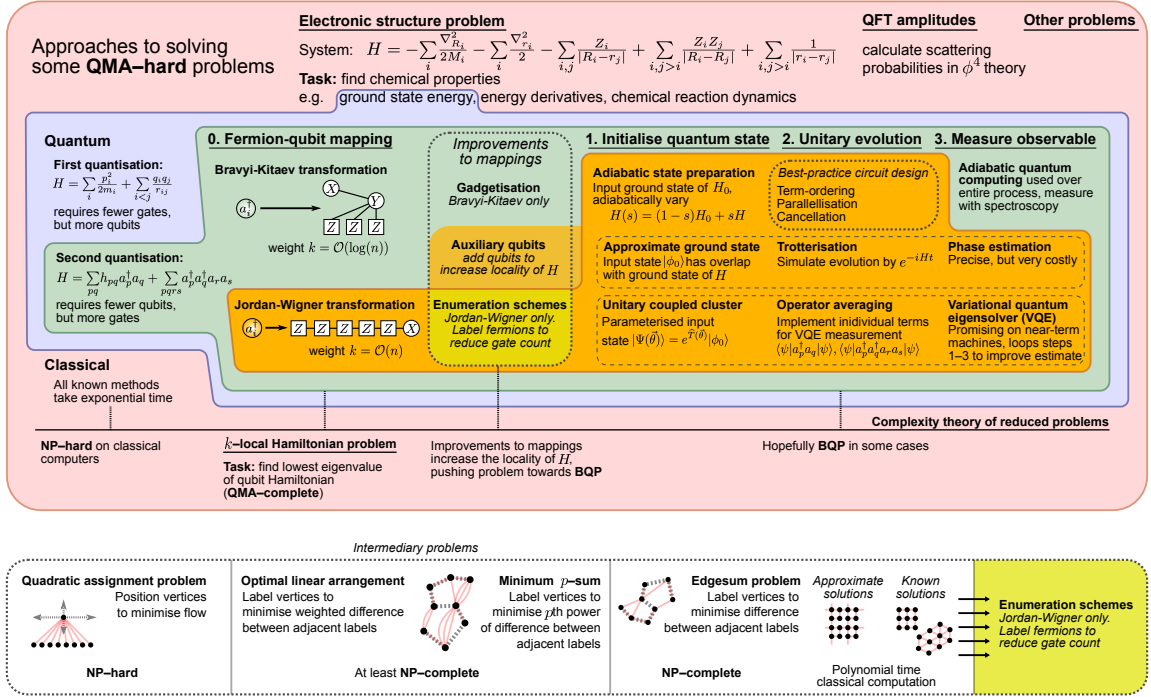


Figure 23: Top: broad overview of the role fermion enumeration plays within quantum algorithms for calculating physical properties, in this case the ground state energy of molecular Hamiltonians. Bottom: overview of the complexity-theoretic classification of the problems that generalize the Edgesum problem, the solutions of which are the optimal fermion enumeration schemes.

The search for more efficient mappings beyond Jordan-Wigner transformation resulted in Bravyi-Kitaev type transformations [25], which lead to exponentially shorter Pauli strings in the asymptotic limit. However, the Bravyi-Kitaev transformation does not outperform Jordan-Wigner on modest fermionic systems and has a similar T-gate count [34]. The Jordan-Wigner mapping has also gained a widespread use because it demands far fewer degrees of connectivity in the qubit architecture [16]. Authors have embedded the  $k$ -local Hamiltonian problems in higher-dimensional Hilbert spaces; through a process called gadgetisation in some BK-based adiabatic quantum computing protocols [6], or through the introduction of auxiliary qubits for both BK [15, 18, 19] and JW-type [16, 35, 12] mappings.

In our work, we introduced optimisation of the Jordan-Wigner transformation via fermion enumeration scheme. Our result leads to a fully optimised Jordan-Wigner transformation in the ancilla-free case, and where the qubits lie on a 1D array. In Section 4.2 we show that our results apply to a variety of qubit architectures.

## 4.2 Compatibility with existing tools

Most of the results that made use of the Jordan-Wigner and Bravyi-Kitaev transformations, rely on qubits with a higher connectivity than the 1D array. In particular, Verstraete and Cirac [12] pursue a Jordan-Wigner type mapping to transform a local Hamiltonian on a fermionic lattice to a local Hamiltonian on a qubit lattice. Subsequent works have followed suit, usually working towards preserving geometric locality between the fermions and qubits, where the assumption is that the qubit architecture is the same as the fermionic graph [15, 35, 16, 19].

Our results are compatible with all existing qubit architectures. To see this, consider for example decomposing Verstraete-Cirac mapping into two components: 1) the *enumeration* of the fermions, which projects the fermionic connectivity graph  $G_F$  onto a 1D array of qubits, and then 2) the *embedding* of the 1D array of qubits into the qubit architecture  $G_Q$ . Figure 24 visualises the distinction between the two processes.

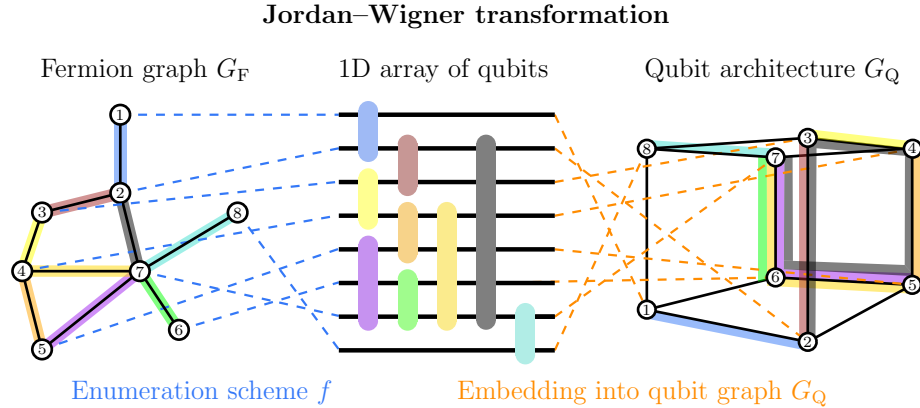


Figure 24: It is important to distinguish the choice of fermion enumeration scheme from the choice of Pauli string embedding. Only the latter is dependent on the qubit architecture.

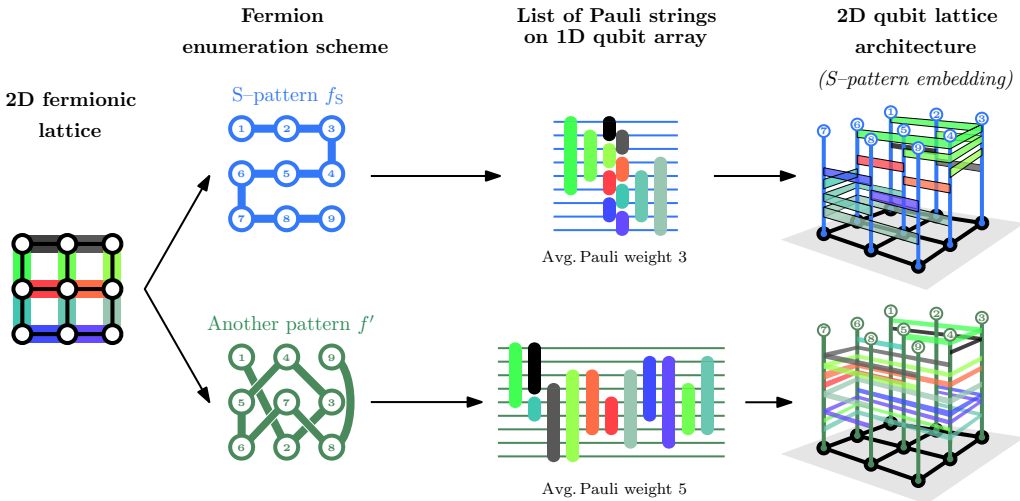


Figure 25: When working with elaborate qubit architectures such as the 2D lattice, the fermion enumeration scheme need not follow the underlying qubit connectivity. This figure highlights the freedom to choose any scheme to enumerate fermions, yielding averages for the Pauli weights independent of the actual qubit connectivity.

Verstraete and Cirac’s approach is to introduce the S-pattern to enumerate the fermions, and an S-pattern embedding to weave Pauli strings into the qubit lattice, as in the top row of Figure 25. In this work we emphasize that these are two entirely separate processes, and the choice of fermion enumeration scheme can be done in an entirely separate way to the method of the embedding process. Indeed, as the second row of Figure 25 shows, the path of the fermion enumeration scheme need not follow the connectivity of the qubit architecture at all to provide a valid mapping.

In conclusion, in order to minimise the average Pauli weight of a Jordan-Wigner type mapping, the enumeration scheme that solves  $G_F$ ’s edgesum problem provides the optimal result, no matter the structure of the qubit architecture that will eventually implement the Pauli strings. Crucially, the improvement to a Jordan-Wigner transformation through the choice of an optimal fermion enumeration scheme comes at the cost of no extra resources. This distinguishes the result from other methods of improving fermion-qubit mappings such as the introduction of auxiliary qubits [12, 16, 15, 35].

It is possible to conceive of metrics for fermion enumeration scheme that do depend on qubit architectures. For example, one could penalise strings of Pauli gates that spread through the graph  $G_Q$  sparsely, and reward clustered Pauli strings. This poses a different problem and the ‘optimal’ enumeration scheme will need to take into account the qubit architecture as well. We expect that this is a much more difficult problem to solve than minimising average Pauli weight through solutions to the Edgesum problem.

### 4.3 The prospect of adding auxiliary qubits

There is a competitive interplay between the qubit- and gate-count resource costs of fermion-qubit mappings. Moll et al. show how to reduce the number of qubits in a Jordan-Wigner mapping at

the cost of introducing more terms into the molecular Hamiltonian [36], thus increasing quantum gate count. Auxiliary qubit mappings [12, 16, 15, 19, 35] show the converse: that by introducing more qubits into a simulation it is possible to vastly simplify the Hamiltonian. Verstraete and Cirac showed that a system combining an  $N \times N$  2D qubit lattice with  $\mathcal{O}(N^2)$  auxiliary qubits can, with only local operations, simulate a fermionic lattice Hamiltonian [12]. That is, rather than producing long strings of Pauli terms that wind around the qubit lattice as in Figure 25, the auxiliary qubit mappings produce operations that act only on a small number adjacent qubits, at the cost of using a larger qubit lattice.

This begs the question as to what is more important: qubit count or gate count? At the current stage it appears that the benefits of minimizing the former are more significant. In the subsequent work [37] we investigate hybrid fermion-qubit mappings that can combine the choice of optimal fermion enumeration scheme with a constant number of auxiliary qubits improve the locality of the mapping.

**Acknowledgements** SS acknowledges support from the Royal Society University Research Fellowship scheme. MC is funded by Cambridge Australia Allen and DAMTP Scholarship and the Royal Society PhD studentship.

## 5 Appendix

### 5.1 Edgesum of S-pattern

**Lemma 7.** On an  $N \times N$  lattice, the S-pattern  $f_S$  has edgesum  $C^1(f_S) = N^3 - N$ .

*Proof.* Figure 26 displays the S-pattern enumeration procedure for an  $N \times N$  grid, as well as the differences between adjacent vertices' indices.

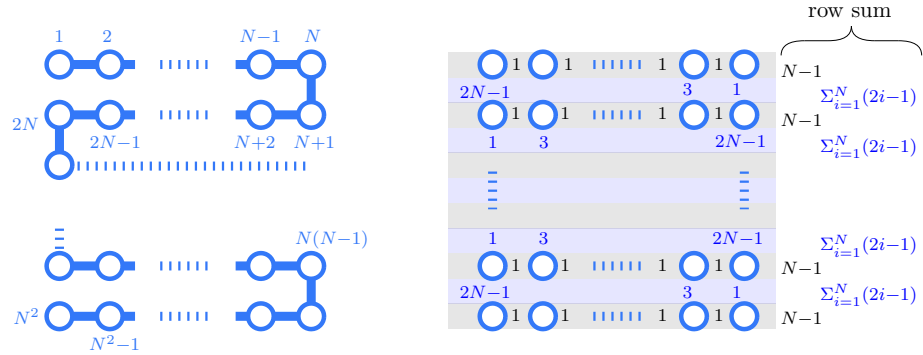


Figure 26: **Left:** S-pattern enumeration on the  $N \times N$  square lattice. **Right:** Differences between vertex labels using the S-pattern enumeration, with row totals on the far right.

Regardless of whether  $N$  is odd or even, the cost is thus

$$C^1(f_S) = (N-1) \times \text{no. of rows} + \sum_{i=1}^N (2i-1) \times (\text{no. of rows} - 1) \quad (63)$$

$$= N^2 - N + (N-1)(N(N+1) - N) \quad (64)$$

$$= N^2 - N - N^2 + N + N(N^2 - 1) \quad (65)$$

$$= N^3 - N. \quad \square$$

The average Pauli weight for the S-pattern on a square lattice is then

$$\text{Avg. Pauli weight} = \frac{C^1(f_S)}{|E|} + 1 = \frac{N^3 - N}{2N(N-1)} + 1 = \frac{1}{2}N + \frac{3}{2}. \quad (66)$$

## References

- [1] Alán Aspuru-Guzik, Anthony D Dutoi, Peter J Love, and Martin Head-Gordon. Simulated quantum computation of molecular energies. *Science*, 309(5741):1704–1707, 2005.
- [2] Jarrod R McClean, Ryan Babbush, Peter J Love, and Alán Aspuru-Guzik. Exploiting locality in quantum computation for quantum chemistry. *The journal of physical chemistry letters*, 5(24):4368–4380, 2014.
- [3] Ivan Kassal, Stephen P Jordan, Peter J Love, Masoud Mohseni, and Alán Aspuru-Guzik. Polynomial-time quantum algorithm for the simulation of chemical dynamics. *Proceedings of the National Academy of Sciences*, 105(48):18681–18686, 2008.
- [4] Ivan Kassal and Alán Aspuru-Guzik. Quantum algorithm for molecular properties and geometry optimization. *The Journal of chemical physics*, 131(22):224102, 2009.
- [5] Gerardo Ortiz, James E Gubernatis, Emanuel Knill, and Raymond Laflamme. Quantum algorithms for fermionic simulations. *Physical Review A*, 64(2):022319, 2001.
- [6] Ryan Babbush, Peter J Love, and Alán Aspuru-Guzik. Adiabatic quantum simulation of quantum chemistry. *Scientific reports*, 4(1):1–11, 2014.
- [7] Hefeng Wang, Sabre Kais, Alán Aspuru-Guzik, and Mark R Hoffmann. Quantum algorithm for obtaining the energy spectrum of molecular systems. *Physical Chemistry Chemical Physics*, 10(35):5388–5393, 2008.
- [8] A Yu Kitaev. Quantum measurements and the abelian stabilizer problem. *arXiv preprint quant-ph/9511026*, 1995.
- [9] Daniel S Abrams and Seth Lloyd. Quantum algorithm providing exponential speed increase for finding eigenvalues and eigenvectors. *Physical Review Letters*, 83(24):5162, 1999.
- [10] Alberto Peruzzo, Jarrod McClean, Peter Shadbolt, Man-Hong Yung, Xiao-Qi Zhou, Peter J Love, Alán Aspuru-Guzik, and Jeremy L O’Brien. A variational eigenvalue solver on a photonic quantum processor. *Nature communications*, 5(1):1–7, 2014.
- [11] Jarrod R McClean, Jonathan Romero, Ryan Babbush, and Alán Aspuru-Guzik. The theory of variational hybrid quantum-classical algorithms. *New Journal of Physics*, 18(2):023023, 2016.
- [12] Frank Verstraete and J Ignacio Cirac. Mapping local hamiltonians of fermions to local Hamiltonians of spins. *Journal of Statistical Mechanics: Theory and Experiment*, 2005(09):P09012, 2005.
- [13] Ivan Kassal, James D Whitfield, Alejandro Perdomo-Ortiz, Man-Hong Yung, and Alán Aspuru-Guzik. Simulating chemistry using quantum computers. *Annual review of physical chemistry*, 62:185–207, 2011.
- [14] Julia Kempe, Alexei Kitaev, and Oded Regev. The complexity of the local hamiltonian problem. *Siam journal on computing*, 35(5):1070–1097, 2006.
- [15] Charles Derby and Joel Klassen. Low weight fermionic encodings for lattice models. *arXiv preprint arXiv:2003.06939*, 2020.

- [16] Mark Steudtner and Stephanie Wehner. Quantum codes for quantum simulation of fermions on a square lattice of qubits. *Physical Review A*, 99(2):022308, 2019.
- [17] Pascual Jordan and Eugene Wigner. Über das Paulische Äquivalenzverbot. *Zeitschrift für Physik*, 47(9-10):631–651, September 1928.
- [18] Kanav Setia, Sergey Bravyi, Antonio Mezzacapo, and James D Whitfield. Superfast encodings for fermionic quantum simulation. *Physical Review Research*, 1(3):033033, 2019.
- [19] Zhang Jiang, Jarrod McClean, Ryan Babbush, and Hartmut Neven. Majorana loop stabilizer codes for error mitigation in fermionic quantum simulations. *Physical Review Applied*, 12(6):064041, 2019.
- [20] Zhang Jiang, Amir Kalev, Wojciech Mruczkiewicz, and Hartmut Neven. Optimal fermion-to-qubit mapping via ternary trees with applications to reduced quantum states learning. *Quantum*, 4:276, June 2020.
- [21] Graeme Mitchison and Richard Durbin. Optimal numberings of an  $N \times N$  array. *SIAM Journal on Algebraic Discrete Methods*, 7(4):571–582, 1986.
- [22] Michael R Garey, David S Johnson, and Larry Stockmeyer. Some simplified NP-complete problems. In *Proceedings of the sixth annual ACM symposium on Theory of computing*, pages 47–63, 1974.
- [23] Michael R Garey, Ronald L Graham, David S Johnson, and Donald Ervin Knuth. Complexity results for bandwidth minimization. *SIAM Journal on Applied Mathematics*, 34(3):477–495, 1978.
- [24] Michael R Garey and David S Johnson. *Computers and Intractability: A Guide to the Theory of NP-Completeness*. W. H. Freeman & Co., USA, 1990.
- [25] Sergey B Bravyi and Alexei Yu Kitaev. Fermionic quantum computation. *Annals of Physics*, 298(1):210–226, 2002.
- [26] Tjalling C Koopmans and Martin Beckmann. Assignment problems and the location of economic activities. *Econometrica: journal of the Econometric Society*, pages 53–76, 1957.
- [27] Steven Bradish Horton. *The optimal linear arrangement problem: algorithms and approximation*. PhD thesis, School of Industrial and Systems Engineering, Georgia Institute of Technology, 1997.
- [28] Martin Juvan and Bojan Mohar. Optimal linear labelings and eigenvalues of graphs. *Discrete Applied Mathematics*, 36(2):153–168, 1992.
- [29] Alan George and Alex Pothen. An analysis of spectral envelope reduction via quadratic assignment problems. *SIAM Journal on Matrix Analysis and Applications*, 18(3):706–732, 1997.
- [30] Greg N Frederickson and Susanne E Hambrusch. Planar linear arrangements of outerplanar graphs. *IEEE transactions on Circuits and Systems*, 35(3):323–333, 1988.
- [31] Yung-Ling Lai and Kenneth Williams. A survey of solved problems and applications on bandwidth, edgesum, and profile of graphs. *Journal of graph theory*, 31(2):75–94, 1999.

- [32] Fan-Rong King Chung. On optimal linear arrangements of trees. *Computers & mathematics with applications*, 10(1):43–60, 1984.
- [33] James B Saxe. Dynamic-programming algorithms for recognizing small-bandwidth graphs in polynomial time. *SIAM Journal on Algebraic Discrete Methods*, 1(4):363–369, 1980.
- [34] Andrew Tranter, Peter J Love, Florian Mintert, and Peter V Coveney. A comparison of the bravyi–kitaev and jordan–wigner transformations for the quantum simulation of quantum chemistry. *Journal of chemical theory and computation*, 14(11):5617–5630, 2018.
- [35] James D Whitfield, Vojtěch Havlíček, and Matthias Troyer. Local spin operators for fermion simulations. *Phys. Rev. A*, 94:030301, Sep 2016.
- [36] Nikolaj Moll, Andreas Fuhrer, Peter Staar, and Ivano Tavernelli. Optimizing qubit resources for quantum chemistry simulations in second quantization on a quantum computer. *Journal of Physics A: Mathematical and Theoretical*, 49(29):295301, 2016.
- [37] To appear.